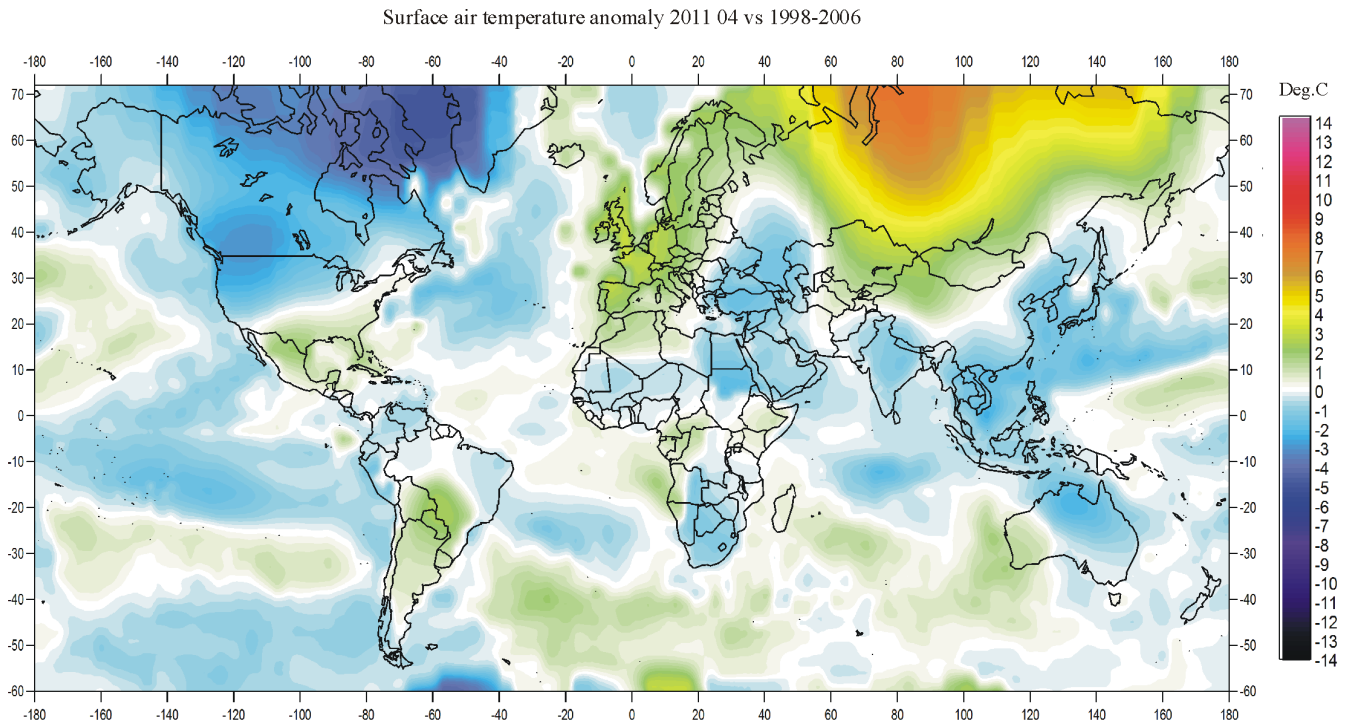


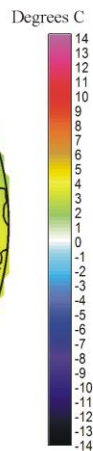
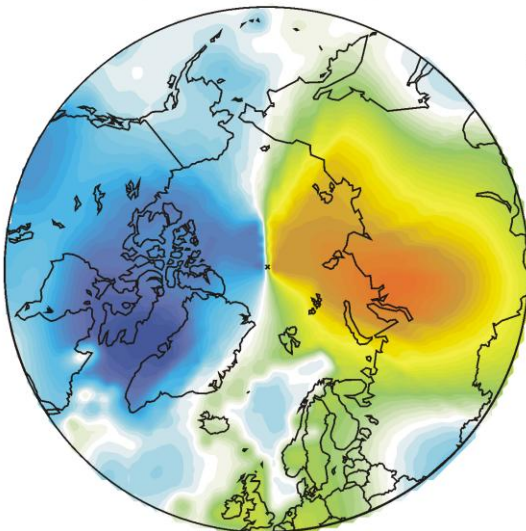
Climate4you update April 2011

www.climate4you.com

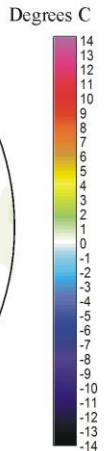
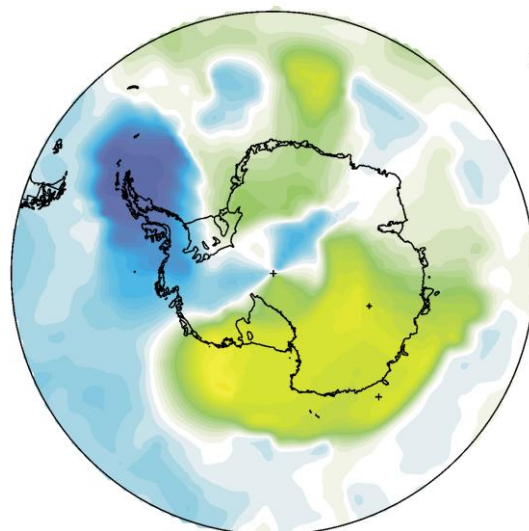
April 2011 global surface air temperature overview



Air temperature 201104 versus average 1998-2006



Air temperature 201104 versus average 1998-2006



April 2011 surface air temperature compared to the average 1998-2006. Green, yellow, red colours indicate areas with higher temperature than the 1998-2006 average, while blue colours indicate lower than average temperatures. Data source: [Goddard Institute for Space Studies \(GISS\)](http://www.giss.nasa.gov)

Comments to the April 2011 global surface air temperature overview

General: This newsletter contains graphs showing a selection of key meteorological variables for April 2011. All temperatures are given in degrees Celsius.

In the above maps showing the geographical pattern of surface air temperatures, the period 1998-2006 is used as reference period. The reason for comparing with this recent period instead of the official WMO 'normal' period 1961-1990, is that the latter period is affected by the relatively cold period 1945-1980. Almost any comparison with such a low average value will therefore appear as high or warm, and it will be difficult to decide if modern surface air temperatures are increasing or decreasing. Comparing with a more recent period overcomes this problem. In addition to this consideration, the recent temperature development suggests that the time window 1998-2006 may roughly represent a global temperature peak. If so, negative temperature anomalies will gradually become more and more widespread as time goes on. However, if positive anomalies instead gradually become more widespread, this reference period only represented a temperature plateau.

In the other diagrams in this newsletter the thin line represents the monthly global average value, and the thick line indicate a simple running average, in most cases a simple moving 37-month average, almost corresponding to three years. The 37-month average is calculated from values covering a range from 18 month before to 18 months after, with equal weight for every month.

The year 1979 has been chosen as starting point in several of the diagrams, as this roughly corresponds to both the beginning of satellite observations and the onset of the late 20th century warming period. Several of the records, however, have a much longer history, which may be inspected on www.Climate4you.com.

Most diagrams shown in this newsletter are also available for download on www.climate4you.com

Global surface air temperatures April 2011 in general was near the 1998-2006 average.

The Northern Hemisphere was characterised by high regional variability. A zone of below average temperatures extended across most of North America. Above average temperatures especially characterised northern Siberia. This positive anomaly and its extension across the Arctic Ocean is the main reason for the increasing global temperature displayed by all surface records (GISS, NCDC and HadCRUT3) for April 2011.

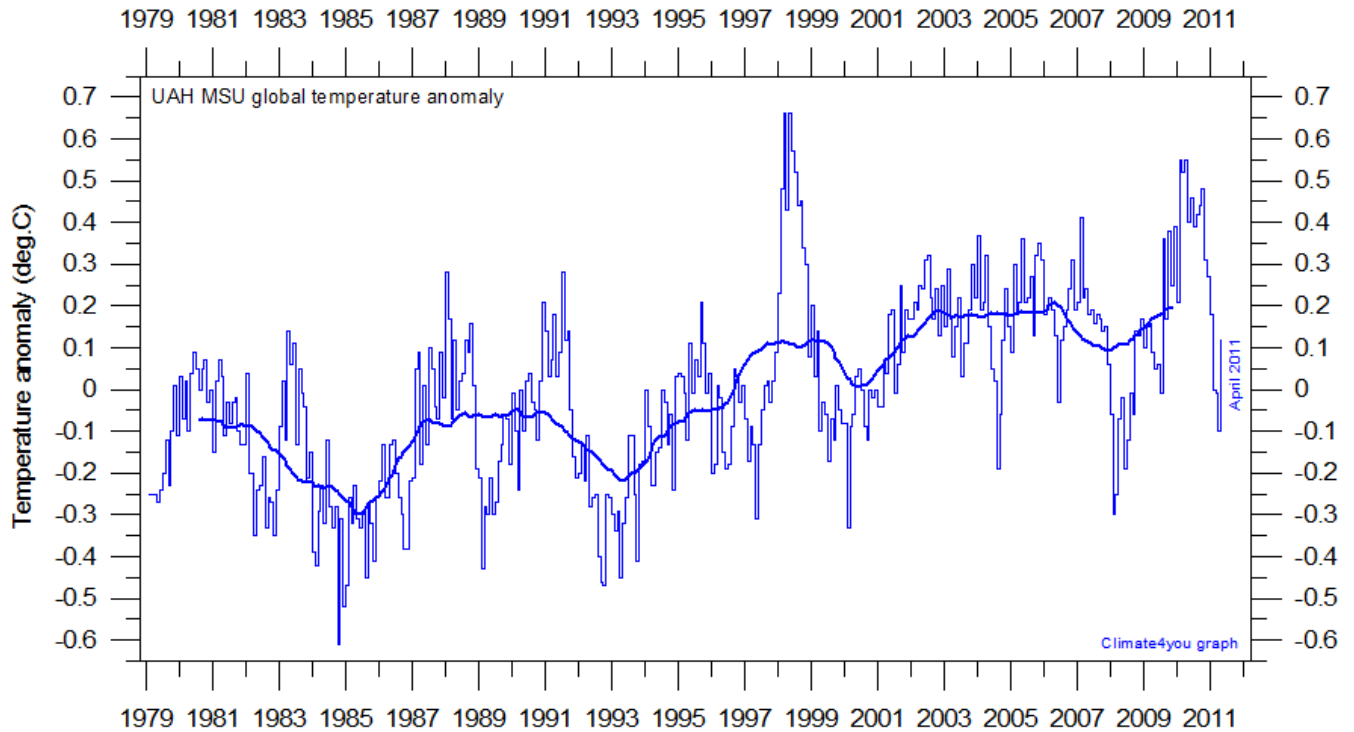
The Southern Hemisphere in general was close to or slightly below average 1998-2006 conditions. Most Africa and Australia experienced below average temperatures, while the picture was more mixed for South America. There were no major warm anomalies in the Southern Hemisphere in April 2011.

Near Equator temperatures conditions were still influenced by the now dwindling La Nina situation. Relatively low temperatures characterised most of the Equatorial regions in the Pacific and Indian Ocean. The Equatorial Atlantic was close to average conditions. Because of the huge areas represented by these regions at low latitudes, the cooling effect on the global average temperature is still felt in April 2011, but to a reduced degree compared to the previous months. The present La Nina situation is presumably coming to an end soon.

The Arctic was characterized by big contrasts as to the surface air temperature. Most areas in Siberia experienced above average 1998-2006 temperatures, while Greenland and the North American Arctic had below average temperatures in April 2011. As in many previous months, the interpolation routine used by GISS is the background for the unrealistic high thermal gradient across the North Pole. This feature is presumably not found in nature, and just represents a interpolation artefact.

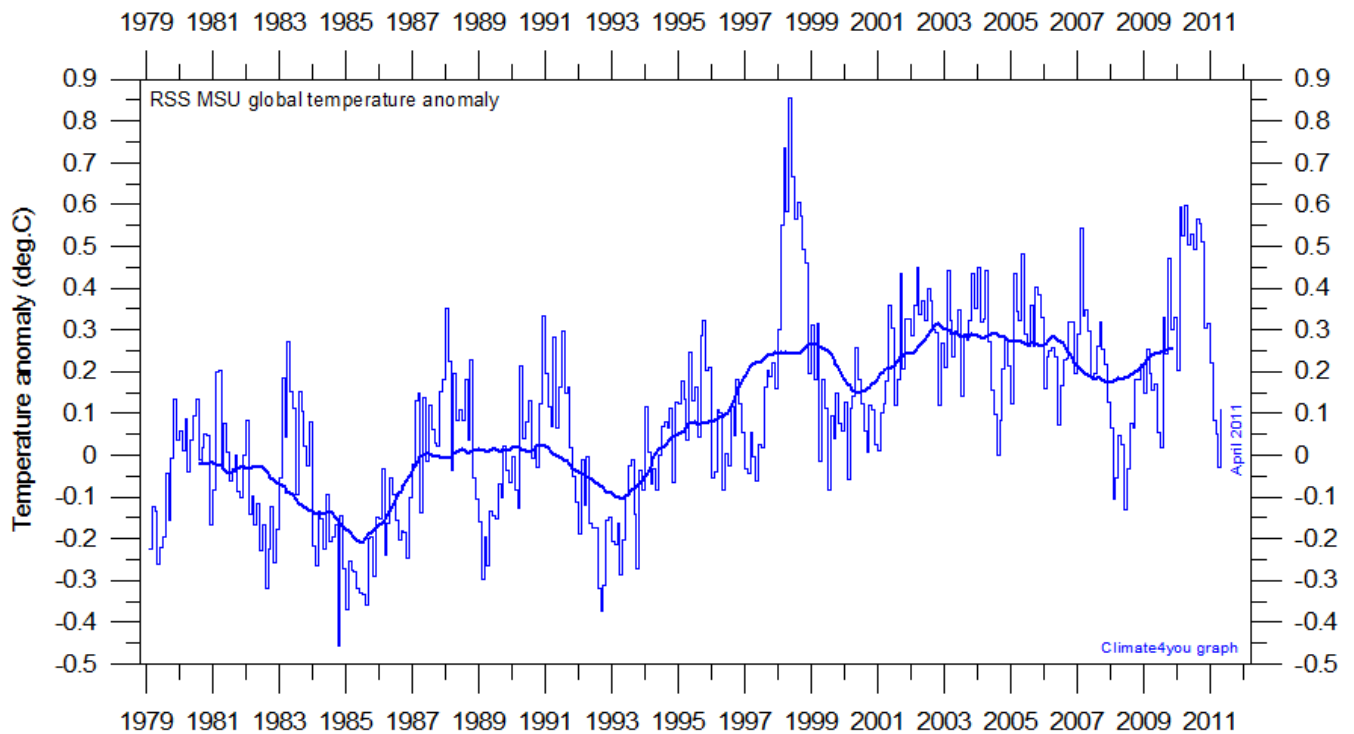
Also the Antarctic displayed contrasts in temperature anomalies. The Antarctic Peninsula had below 1998-2006 average temperatures, while large areas of East Antarctica had above normal temperatures.

Lower troposphere temperature from satellites, updated to April 2011



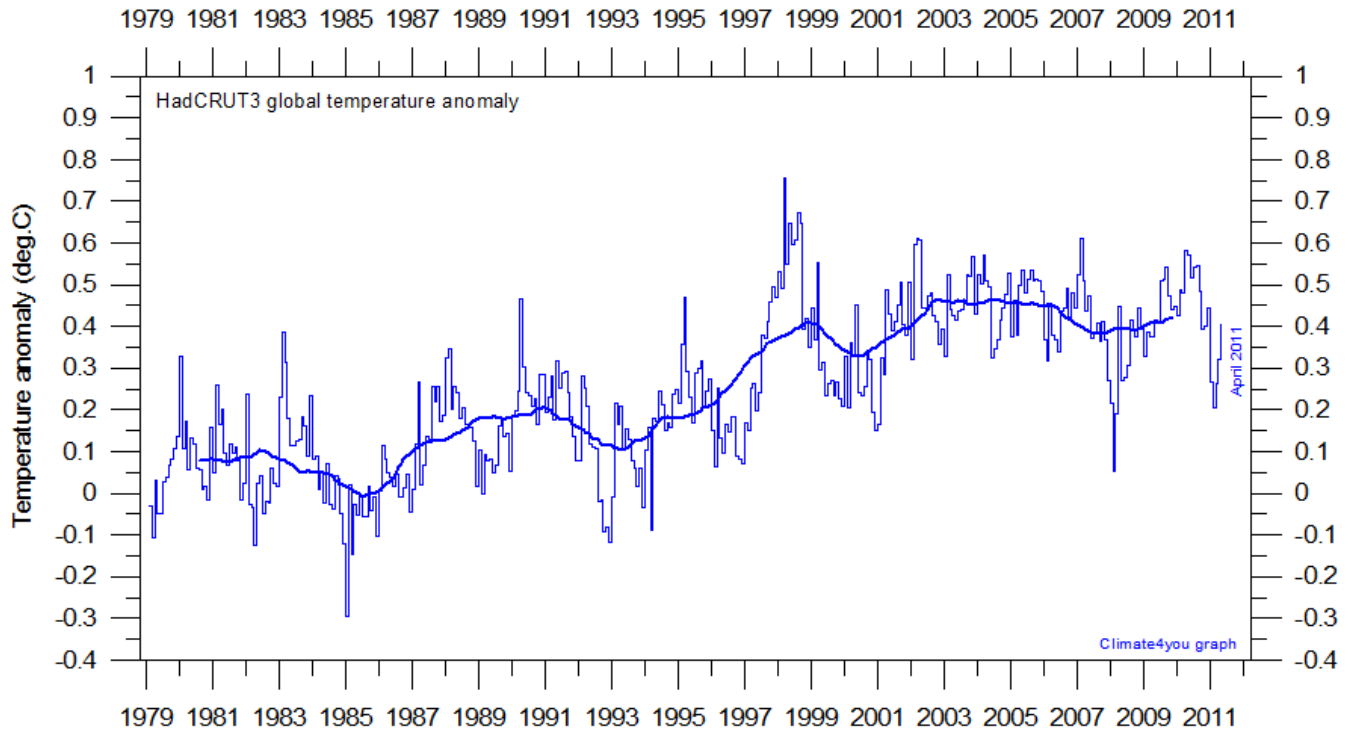
Global monthly average lower troposphere temperature (thin line) since 1979 according to [University of Alabama](#) at Huntsville, USA. The thick line is the simple running 37 month average.

3



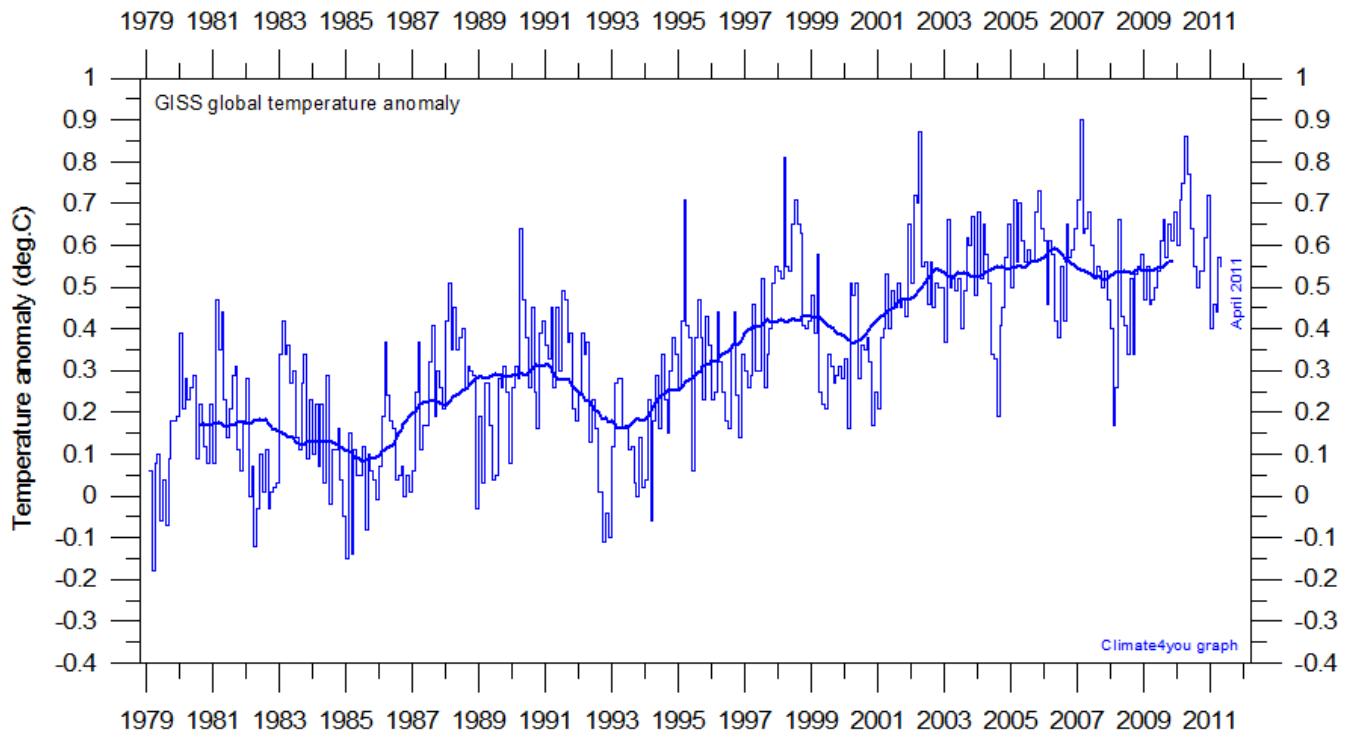
Global monthly average lower troposphere temperature (thin line) since 1979 according to according to [Remote Sensing Systems](#) (RSS), USA. The thick line is the simple running 37 month average.

Global surface air temperature, updated to April 2011

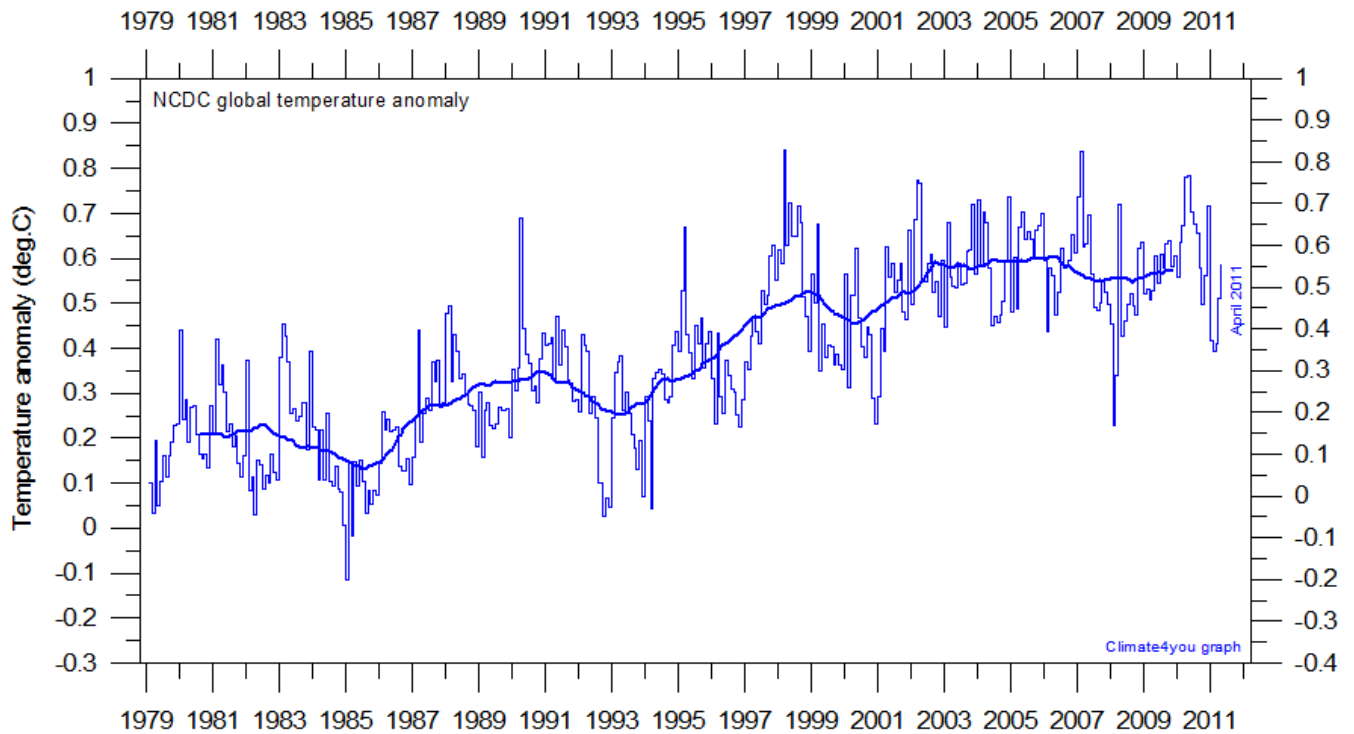


Global monthly average surface air temperature (thin line) since 1979 according to according to the Hadley Centre for Climate Prediction and Research and the University of East Anglia's [Climatic Research Unit \(CRU\)](#), UK. The thick line is the simple running 37 month average.

4



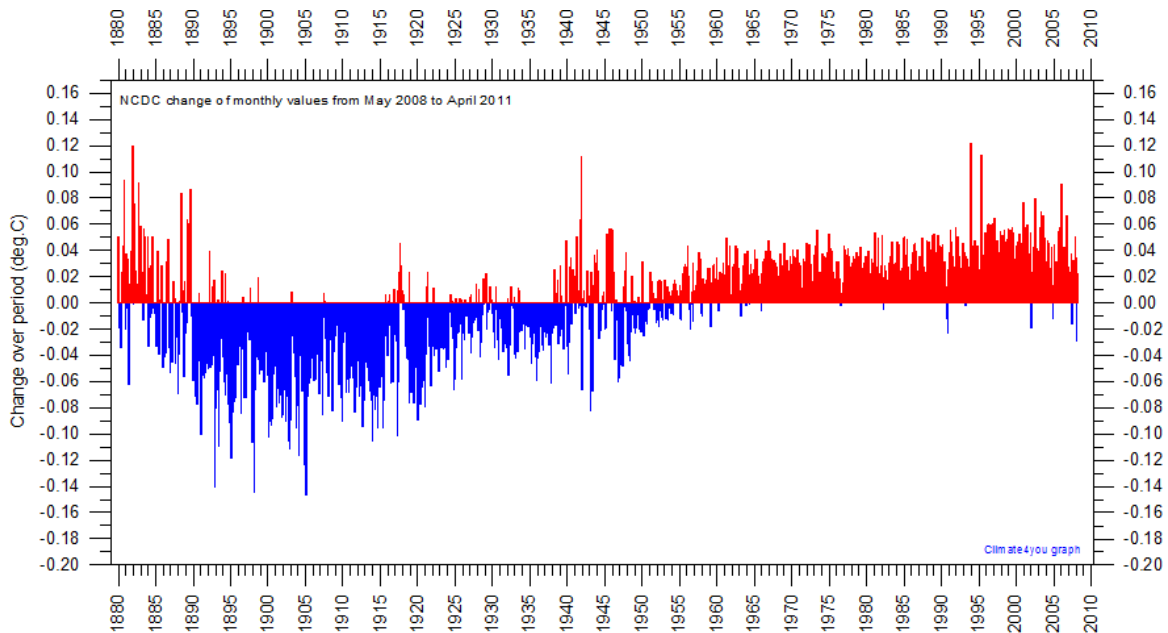
Global monthly average surface air temperature (thin line) since 1979 according to according to the [Goddard Institute for Space Studies \(GISS\)](#), at Columbia University, New York City, USA. The thick line is the simple running 37 month average.



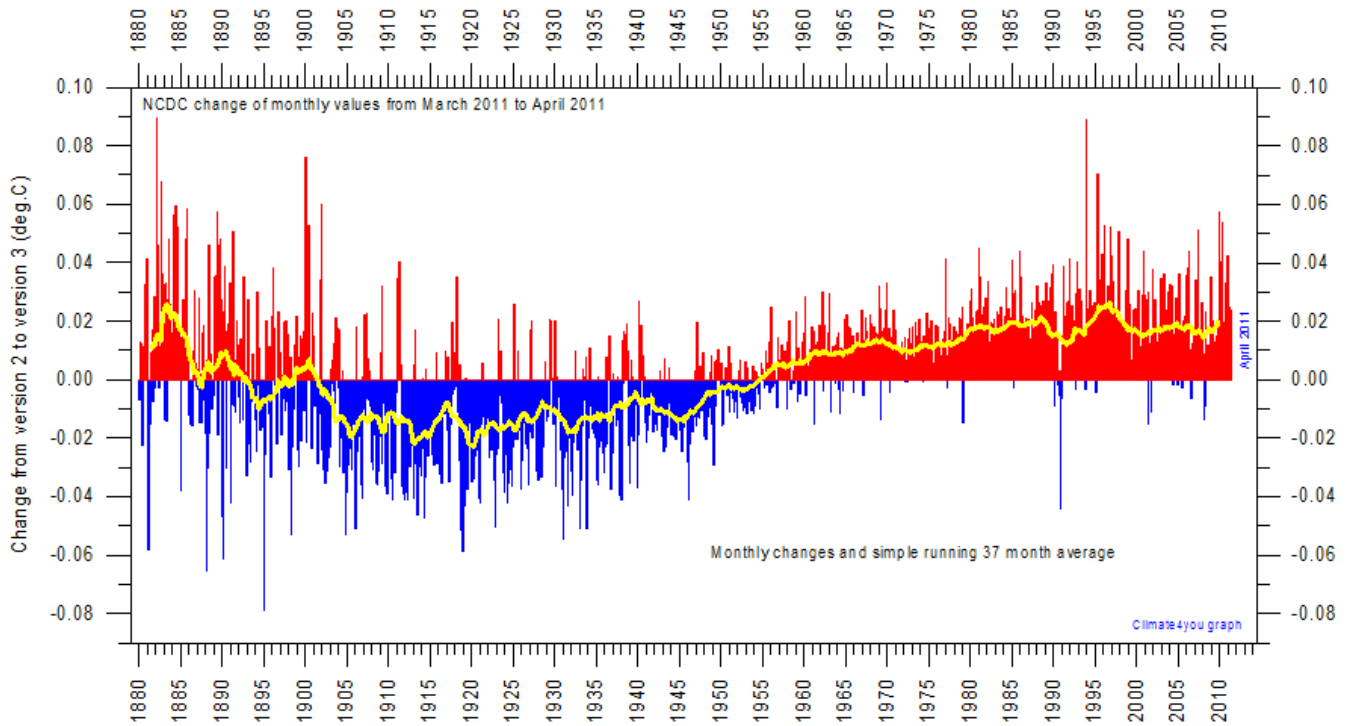
Global monthly average surface air temperature since 1979 according to according to the [National Climatic Data Center](http://www.ncdc.noaa.gov) (NCDC), USA. The thick line is the simple running 37 month average.

5

Some readers have noted that the above temperature estimates display changes when one compare with previous issues of this newsletter, not only for the most recent months, but actually for all months back to the beginning of the record. As an example, the net change of the NCDC record since 17 May 2008 is shown below. By this administrative effort the apparent global temperature increase since 1900 has been enhanced about 0.1°C, or about 14% of the total increase recorded since 1900 by NCDC. The interested reader may find more on this lack of temporal stability on www.climate4you (go to: Global Temperature and then Temporal Stability).



It should be noted that on May 2, 2011, NCDC transitioned to GHCN-M version 3 as the official land component of its global temperature monitoring efforts. GHCN-M version 2 mean temperature dataset will continue to be updated through May 30, 2011, but no support for this version of the dataset will be provided. The net effect of the change from version 2 to 3 can be seen in the diagram below.

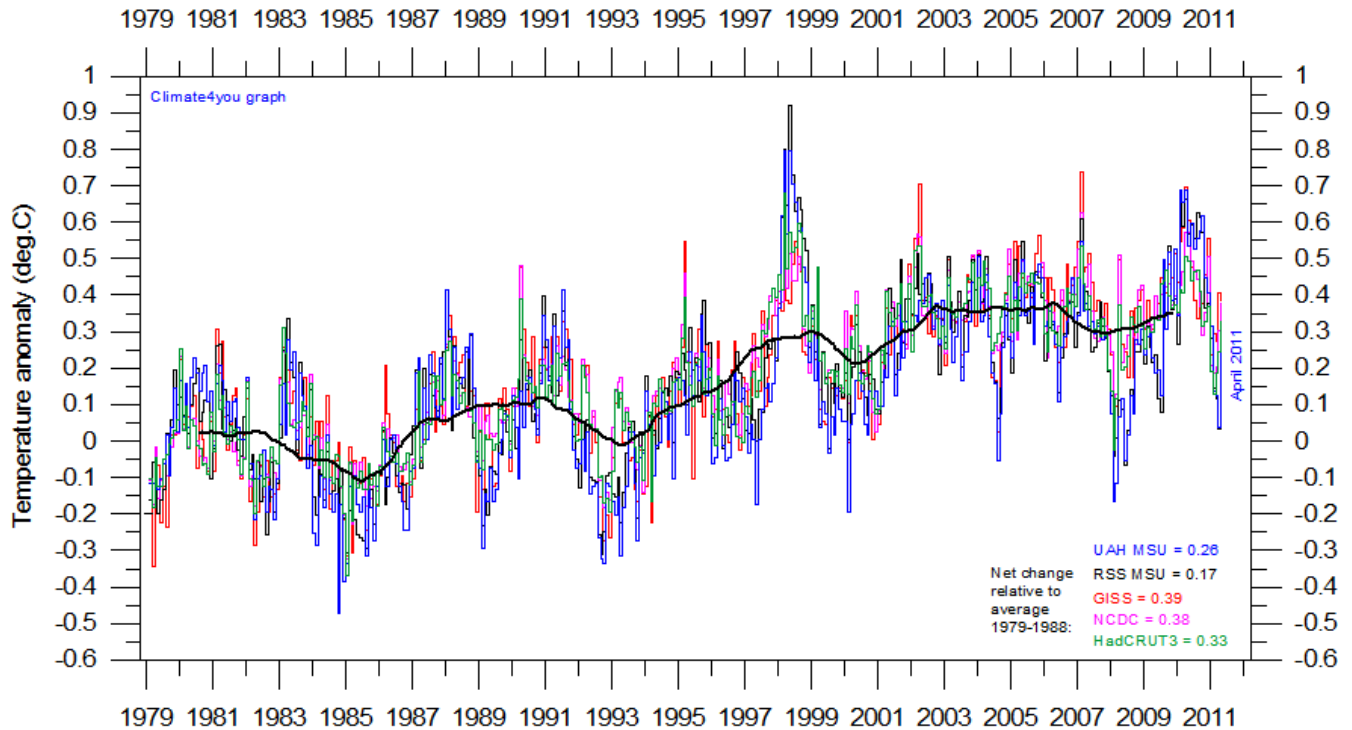


6

Net temperature effect of the 2 May 2011 transition from GHCN-M version 2 to version 3 as the official land component of its global temperature monitoring efforts. The vertical lines indicate the net effect of the version change on monthly temperature values, and the yellow line shows the effect on the simple running 37 month average, nearly corresponding to 3 years.

The overall net effect of the NCDC transition from GHCN-M version 2 to version 3 is to increase global temperatures before 1900, to decrease them between 1900 and 1950, and to increase temperatures after 1950. By this the 20th century temperature rise is about 0.04°C larger in the new version 3 compared to the previous version 2.

All in one, updated to April 2011



7

Superimposed plot of all five global monthly temperature estimates shown above. As the base period differs for the different temperature estimates, they have all been normalised by comparing to the average value of their initial 120 months (10 years) from January 1979 to December 1988. The heavy black line represents the simple running 37 month (c. 3 year) mean of the average of all five temperature records. The numbers shown in the lower right corner represent the temperature anomaly relative to the above mentioned 10 yr average.

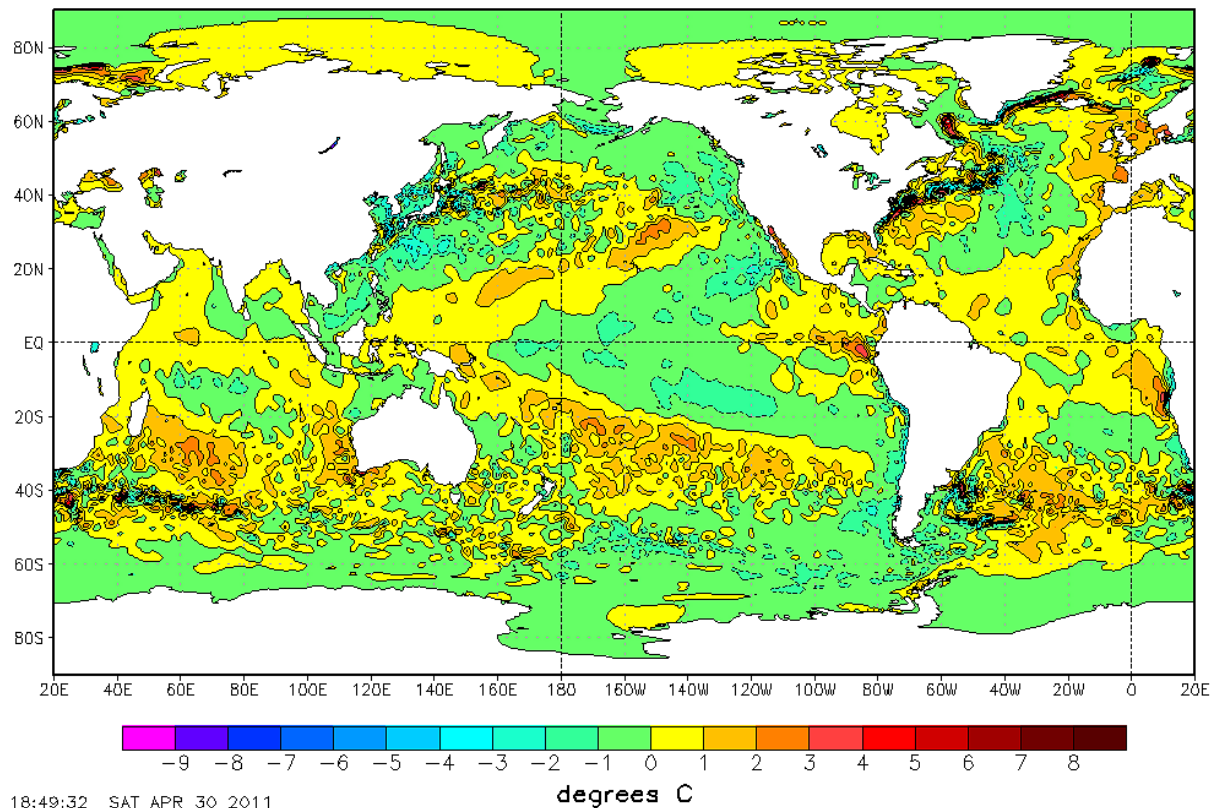
It should be kept in mind that satellite- and surface-based temperature estimates are derived from different types of measurements, and that comparing them directly as done in the diagram above therefore in principle is problematical. However, as both types of estimate often are discussed together, the above diagram may nevertheless be of some interest. In fact, the different types of temperature estimates appear to agree quite well as to the overall temperature variations on a 2-3 year scale, although on a short time scale there may be considerable differences.

All five global temperature estimates presently show stagnation, at least since 2002. There has been no increase in global air temperature since 1998, which was affected by the oceanographic El Niño event. This does not exclude the possibility that global temperatures will begin to increase again later. On the other hand, it also remain a possibility that Earth just now is passing a temperature peak, and that global temperatures will begin to decrease within the coming years. Time will show which of these two possibilities is correct.

Global sea surface temperature, updated to end of April 2011

NOAA/NWS/NCEP/EMC Marine Modeling and Analysis Branch

RTG_SST Anomaly (0.5 deg X 0.5 deg) for 30 Apr 2011

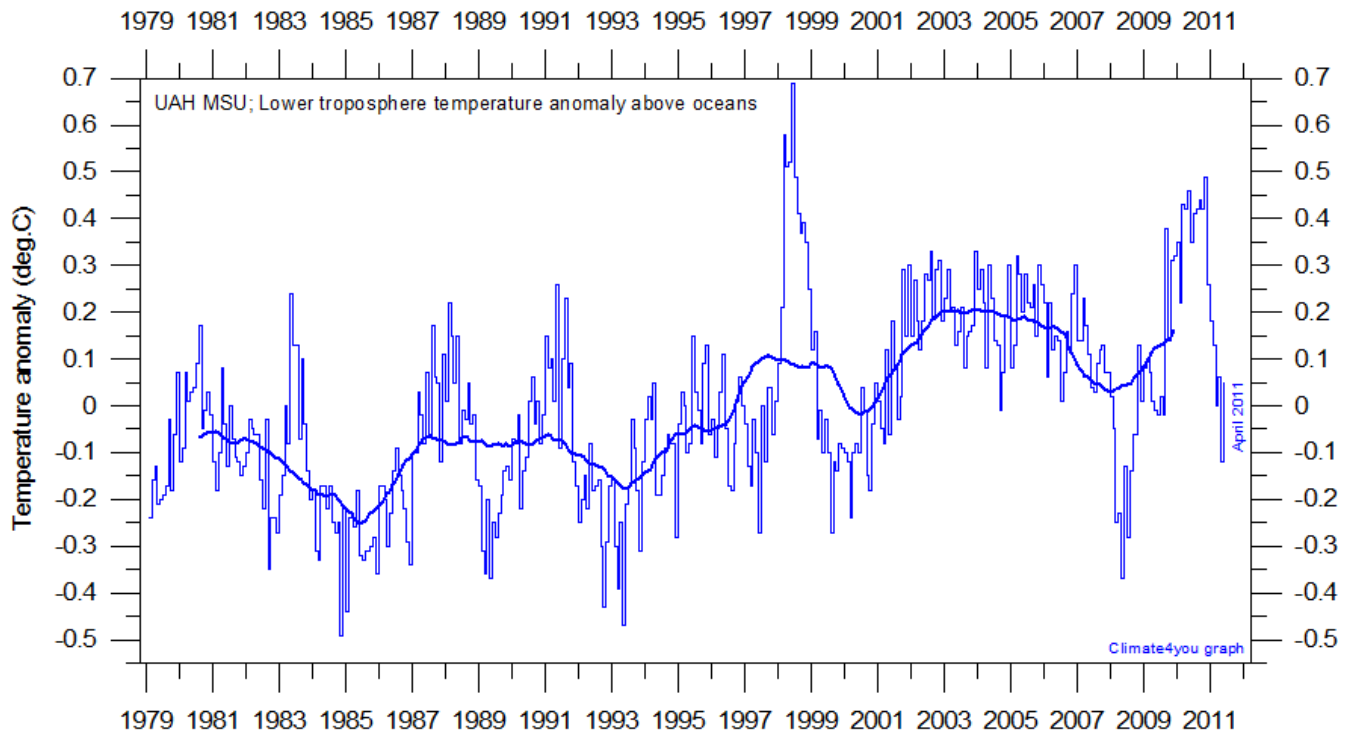


8

Sea surface temperature anomaly at 31 March 2011. Map source: National Centers for Environmental Prediction (NOAA).

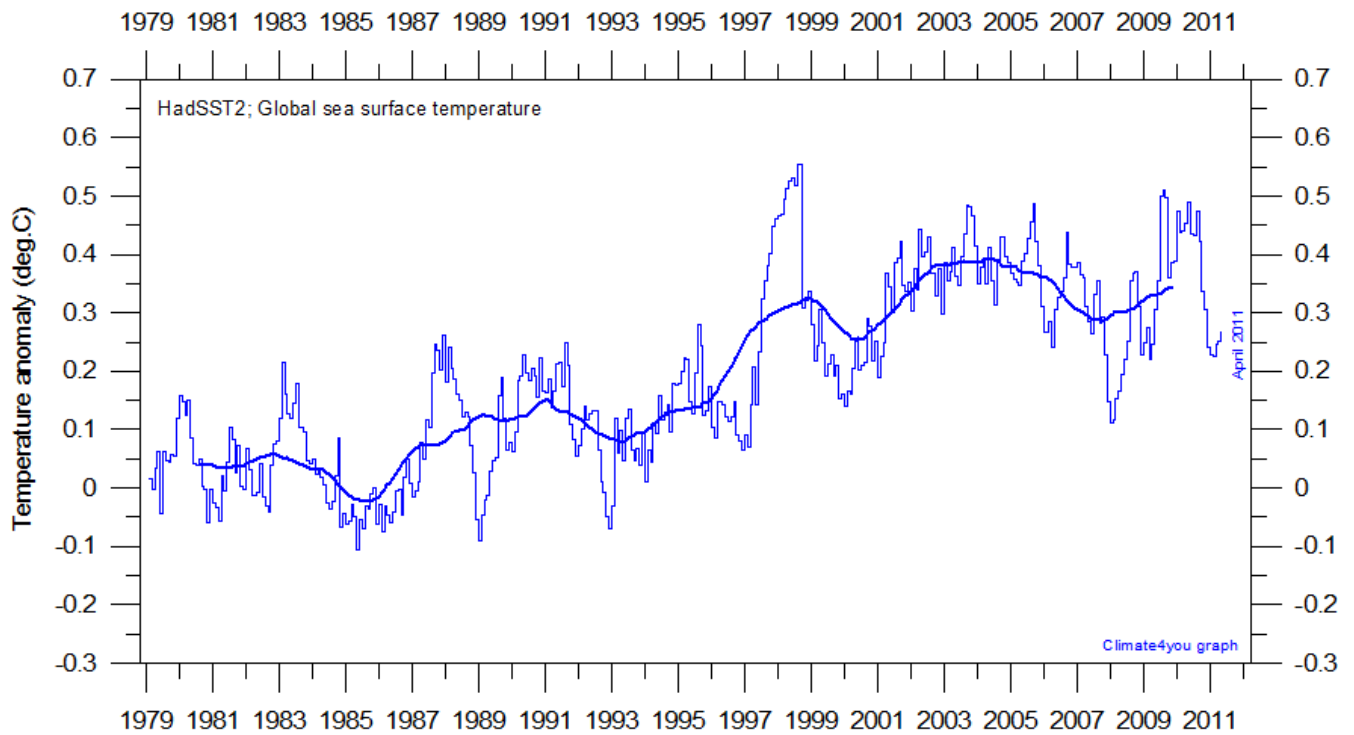
The relative cold surface water dominating the regions near Equator in the Pacific Ocean represents the now dwindling La Niña situation and affects the temperature of the atmosphere above. Because of the large surface areas involved (being near Equator) this natural cyclic development is at the moment affecting the global atmospheric temperature.

However, the significance of any such cooling or warming seen in surface air temperatures should not be overstated. Whenever Earth experiences cold La Niña or warm El Niño episodes major heat exchanges takes place between the Pacific Ocean and the atmosphere above, eventually showing up in estimates of the global air temperature. This does not, however, reflect similar changes in the total heat content of the atmosphere-ocean system. In fact, net changes may be small, as it mainly reflects a redistribution of energy. What matters is the overall development when seen over some years.

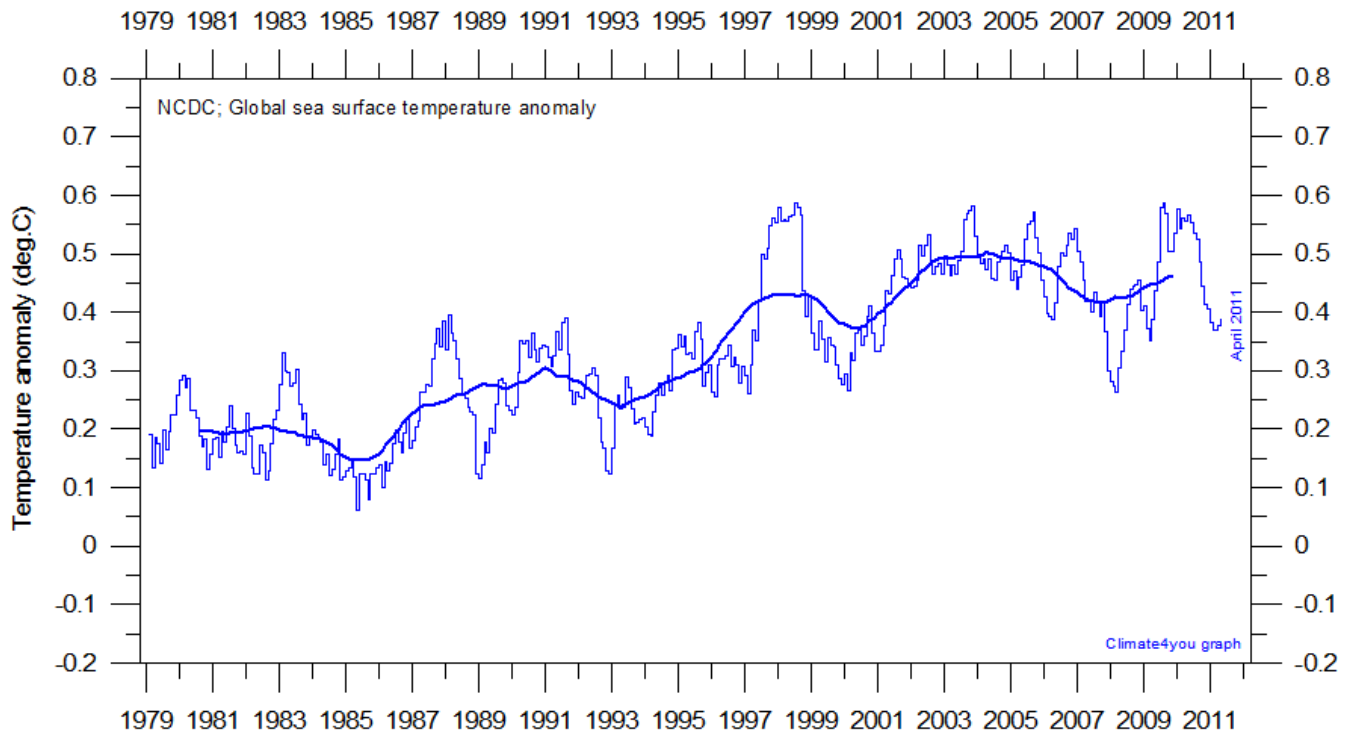


Global monthly average lower troposphere temperature over oceans (thin line) since 1979 according to [University of Alabama](#) at Huntsville, USA. The thick line is the simple running 37 month average.

9

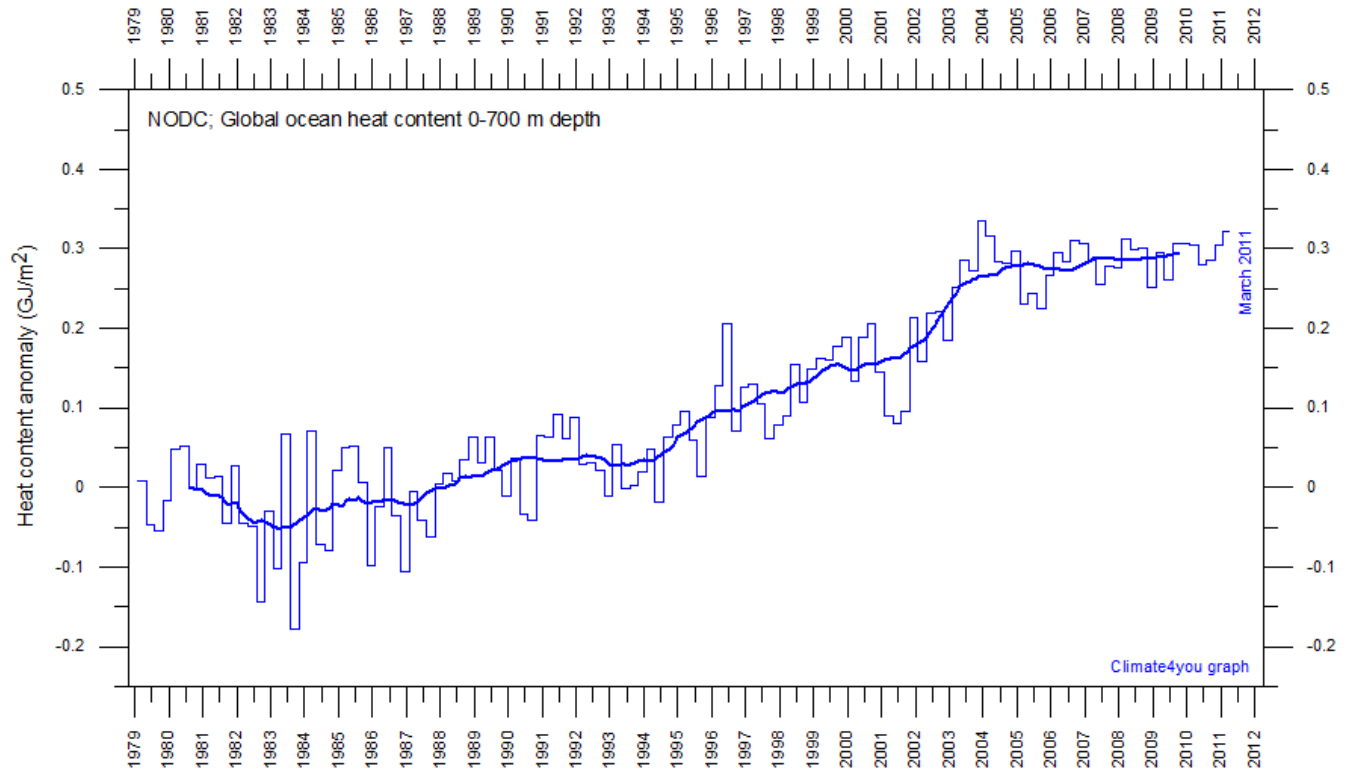


Global monthly average sea surface temperature since 1979 according to University of East Anglia's [Climatic Research Unit \(CRU\)](#), UK. Base period: 1961-1990. The thick line is the simple running 37 month average



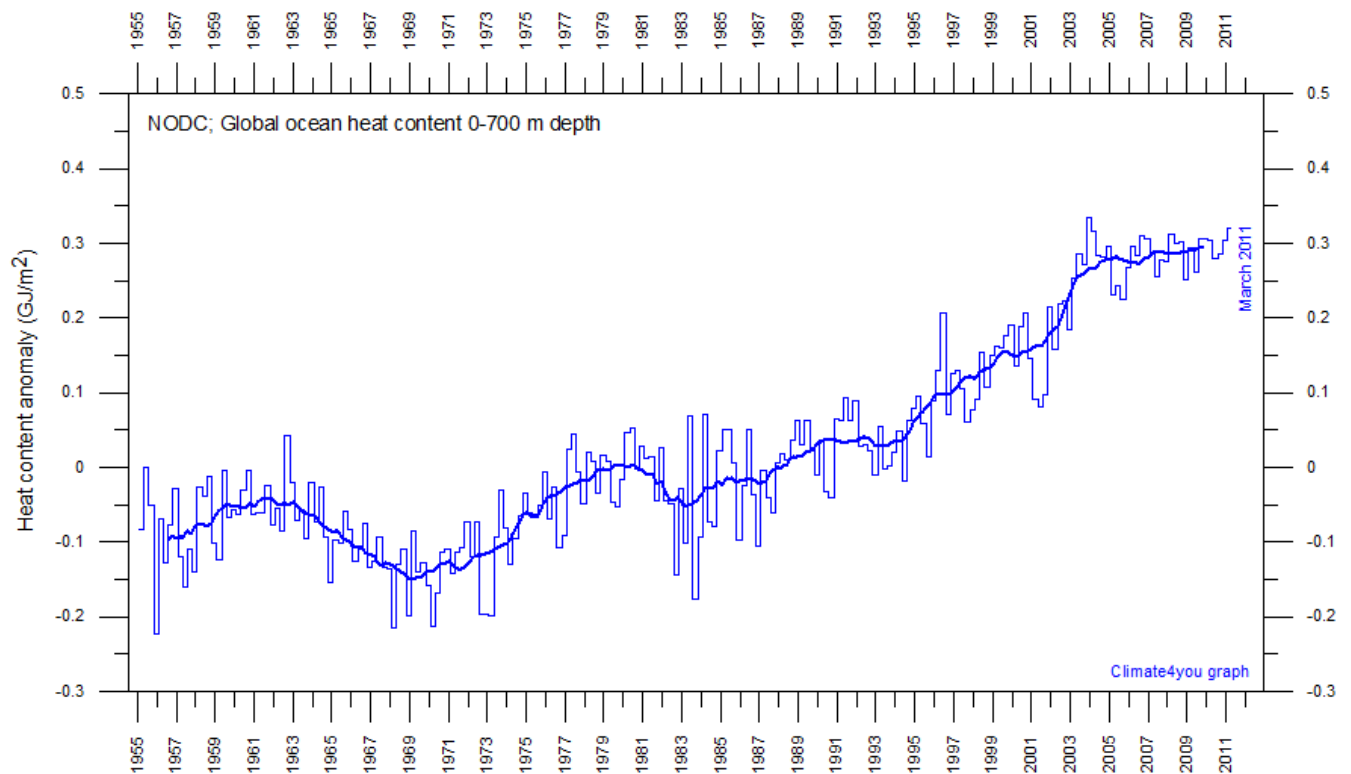
Global monthly average sea surface temperature since 1979 according to the [National Climatic Data Center \(NCDC\)](#), USA. Base period: 1901-2000. The thick line is the simple running 37 month average.

Global ocean heat content, updated to March 2011



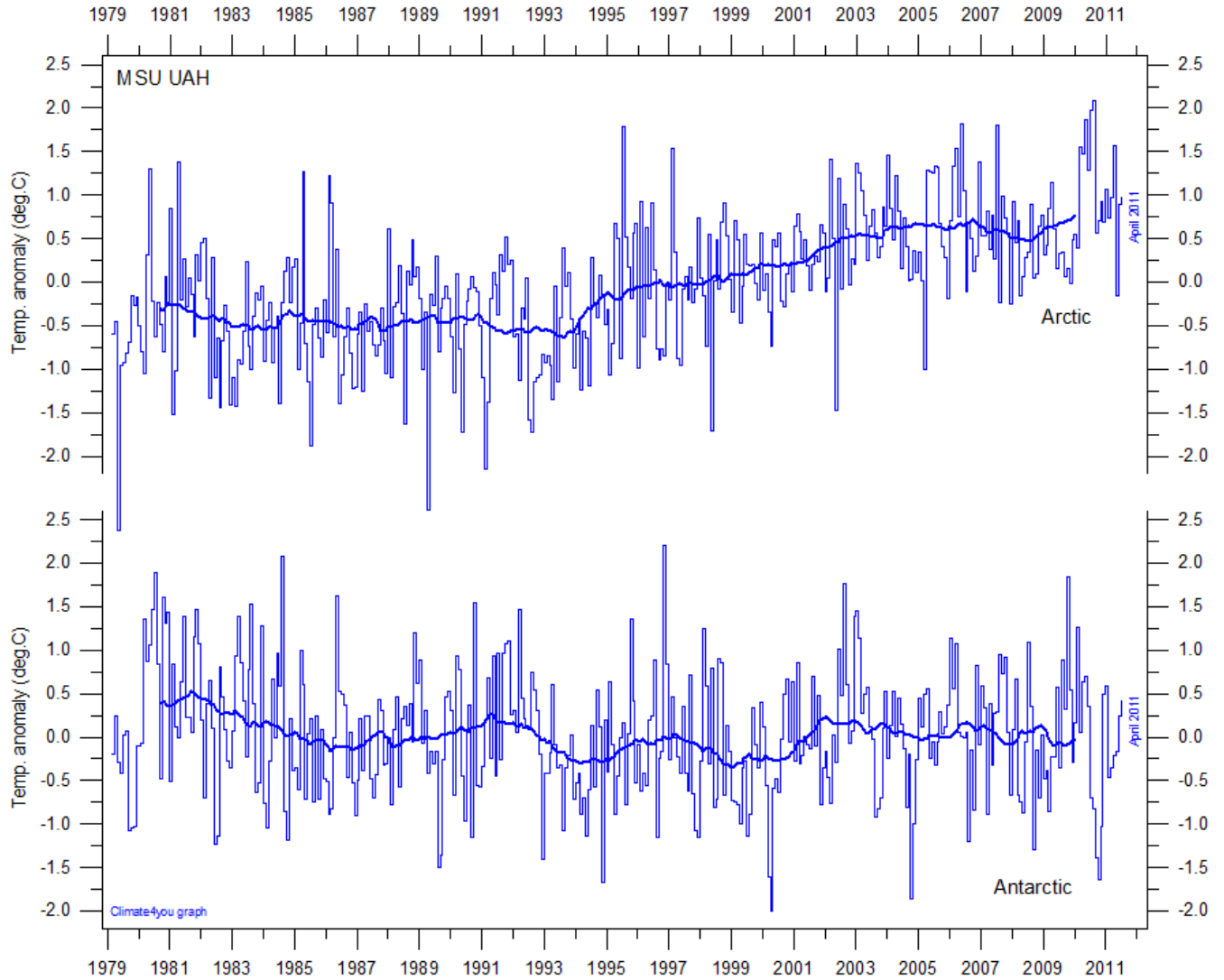
Global monthly heat content anomaly (GJ/m²) in the uppermost 700 m of the oceans since January 1979. Data source: National Oceanographic Data Center(NODC).

11



Global monthly heat content anomaly (GJ/m²) in the uppermost 700 m of the oceans since January 1955. Data source: National Oceanographic Data Center(NODC).

Arctic and Antarctic lower troposphere temperature, updated to April 2011



Global monthly average lower troposphere temperature since 1979 for the North Pole and South Pole regions, based on satellite observations ([University of Alabama](http://www.cgd.cba.uah.edu) at Huntsville, USA). The thick line is the simple running 37 month average, nearly corresponding to a running 3 yr average.

Arctic and Antarctic surface air temperature, updated to March 2011

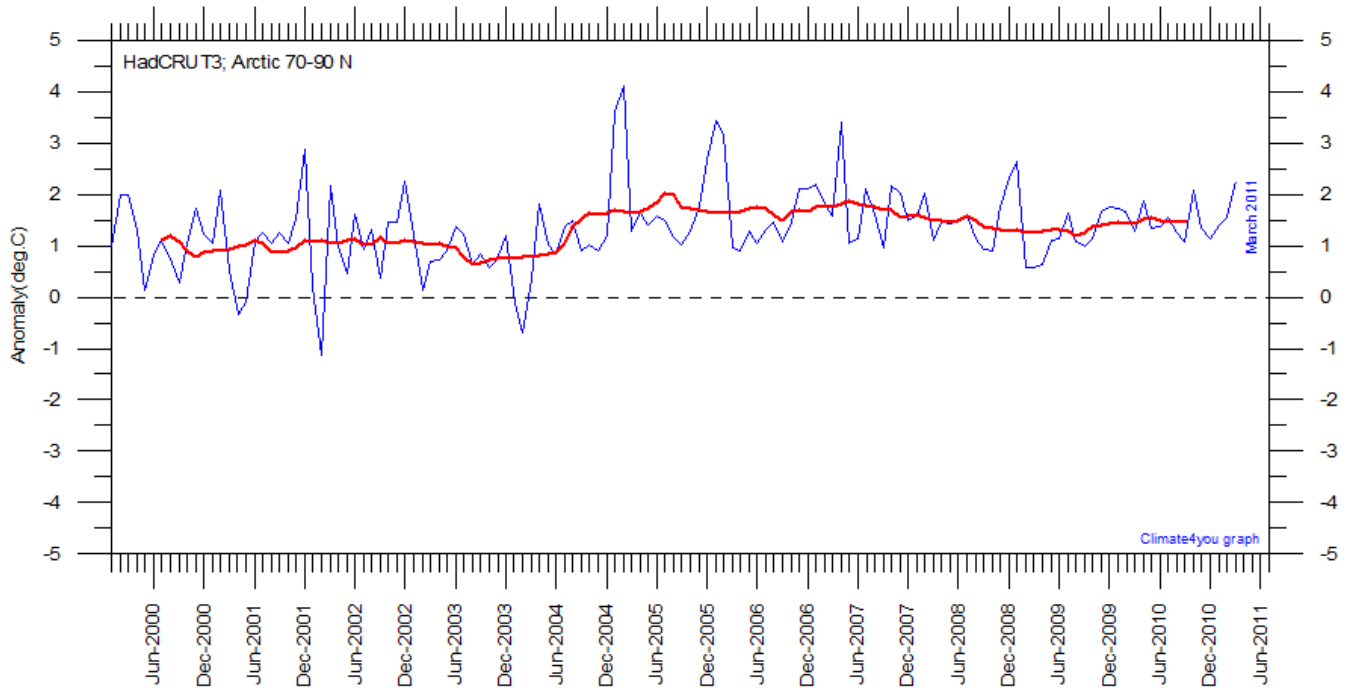


Diagram showing Arctic monthly surface air temperature anomaly 70-90°N since January 2000, in relation to the WMO reference “normal” period 1961-1990. The thin blue line shows the monthly temperature anomaly, while the thicker red line shows the running 13 month average. Data provided by the Hadley Centre for Climate Prediction and Research and the University of East Anglia's [Climatic Research Unit \(CRU\)](#), UK.

13

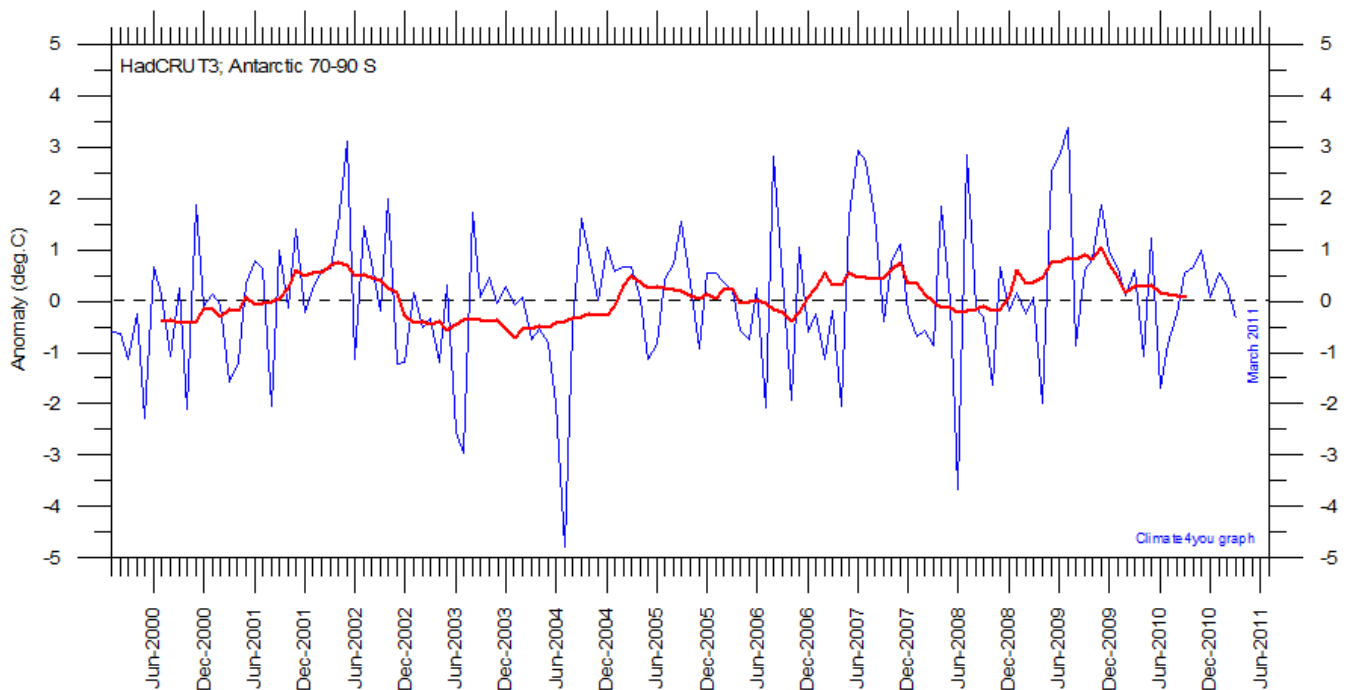


Diagram showing Antarctic monthly surface air temperature anomaly 70-90°S since January 2000, in relation to the WMO reference “normal” period 1961-1990. The thin blue line shows the monthly temperature anomaly, while the thicker red line shows the running 13 month average. Data provided by the Hadley Centre for Climate Prediction and Research and the University of East Anglia's [Climatic Research Unit \(CRU\)](#), UK.

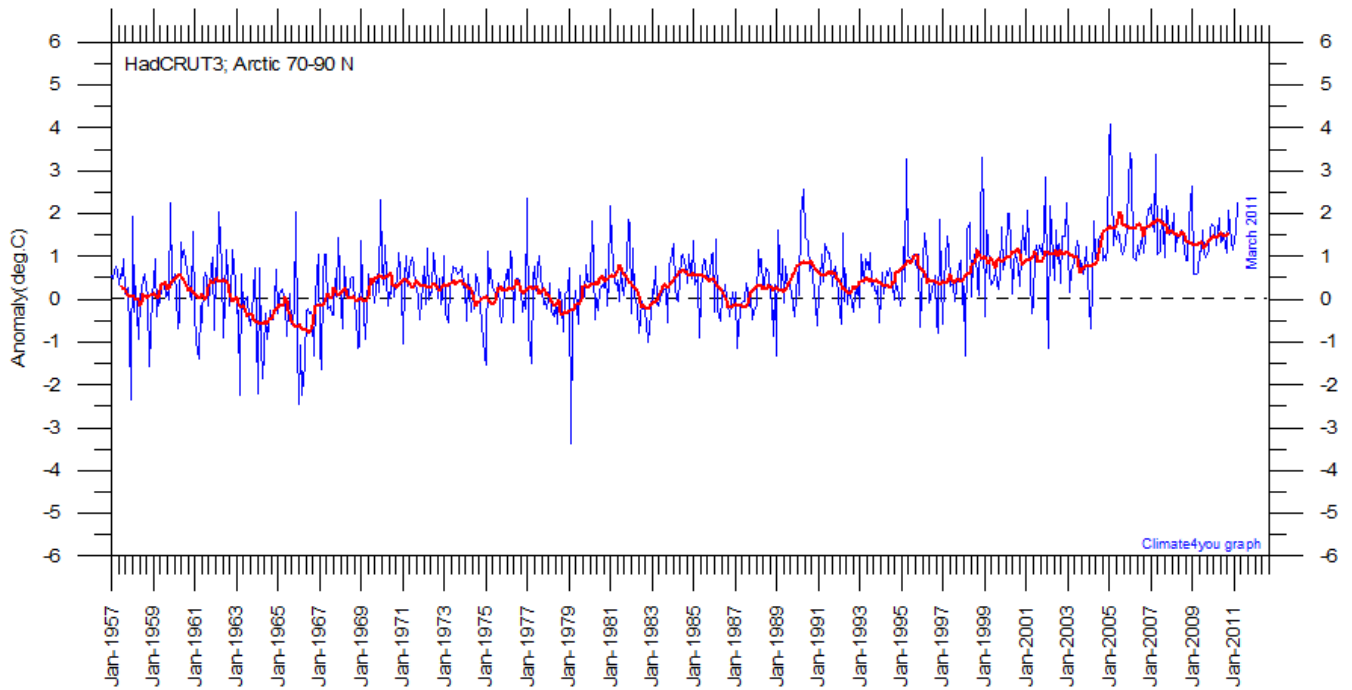


Diagram showing Arctic monthly surface air temperature anomaly 70-90°N since January 1957, in relation to the WMO reference “normal” period 1961-1990. The year 1957 has been chosen as starting year, to ensure easy comparison with the maximum length of the realistic Antarctic temperature record shown below. The thin blue line shows the monthly temperature anomaly, while the thicker red line shows the running 13 month average. Data provided by the Hadley Centre for Climate Prediction and Research and the University of East Anglia's [Climatic Research Unit \(CRU\)](#), UK.

14

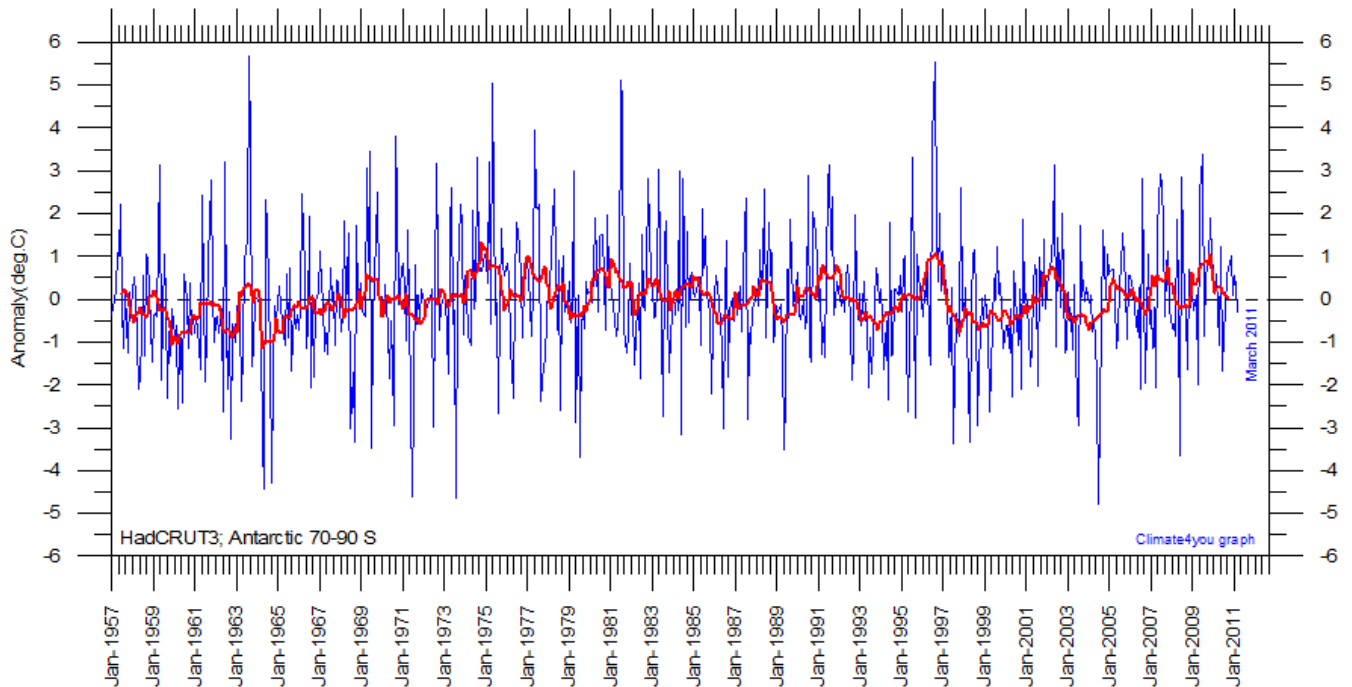


Diagram showing Antarctic monthly surface air temperature anomaly 70-90°S since January 1957, in relation to the WMO reference “normal” period 1961-1990. The year 1957 was an international geophysical year, and several meteorological stations were established in the Antarctic because of this. Before 1957, the meteorological coverage of the Antarctic continent is poor. The thin blue line shows the monthly temperature anomaly, while the thicker red line shows the running 13 month average. Data provided by the Hadley Centre for Climate Prediction and Research and the University of East Anglia's [Climatic Research Unit \(CRU\)](#), UK.

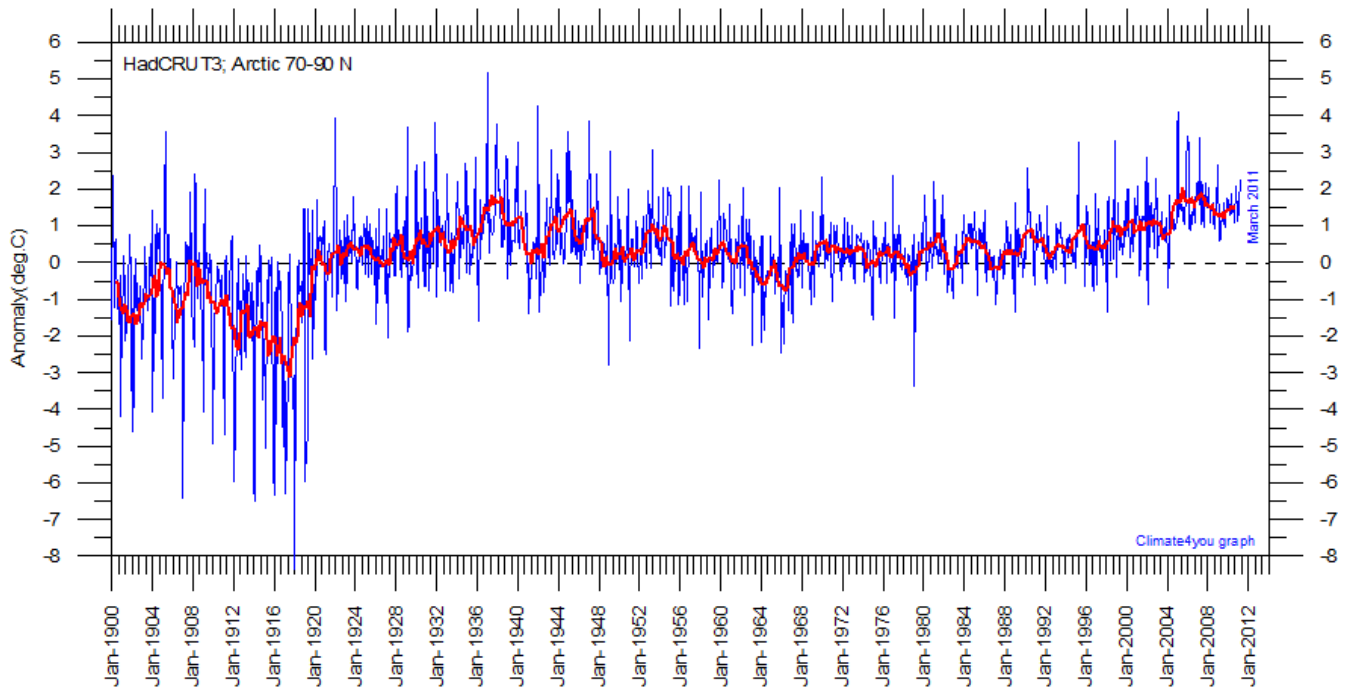


Diagram showing Arctic monthly surface air temperature anomaly 70-90°N since January 1900, in relation to the WMO reference “normal” period 1961-1990. The thin blue line shows the monthly temperature anomaly, while the thicker red line shows the running 13 month average. In general, the range of monthly temperature variations decreases throughout the first 30-50 years of the record, reflecting the increasing number of meteorological stations north of 70°N over time. Especially the period from about 1930 saw the establishment of many new Arctic meteorological stations, first in Russia and Siberia, and following the 2nd World War, also in North America. Because of the relatively small number of stations before 1930, details in the early part of the Arctic temperature record should not be over interpreted. The rapid Arctic warming around 1920 is, however, clearly visible, and is also documented by other sources of information. The period since 2000 is warm, about as warm as the period 1930-1940. Data provided by the Hadley Centre for Climate Prediction and Research and the University of East Anglia's [Climatic Research Unit \(CRU\)](#), UK

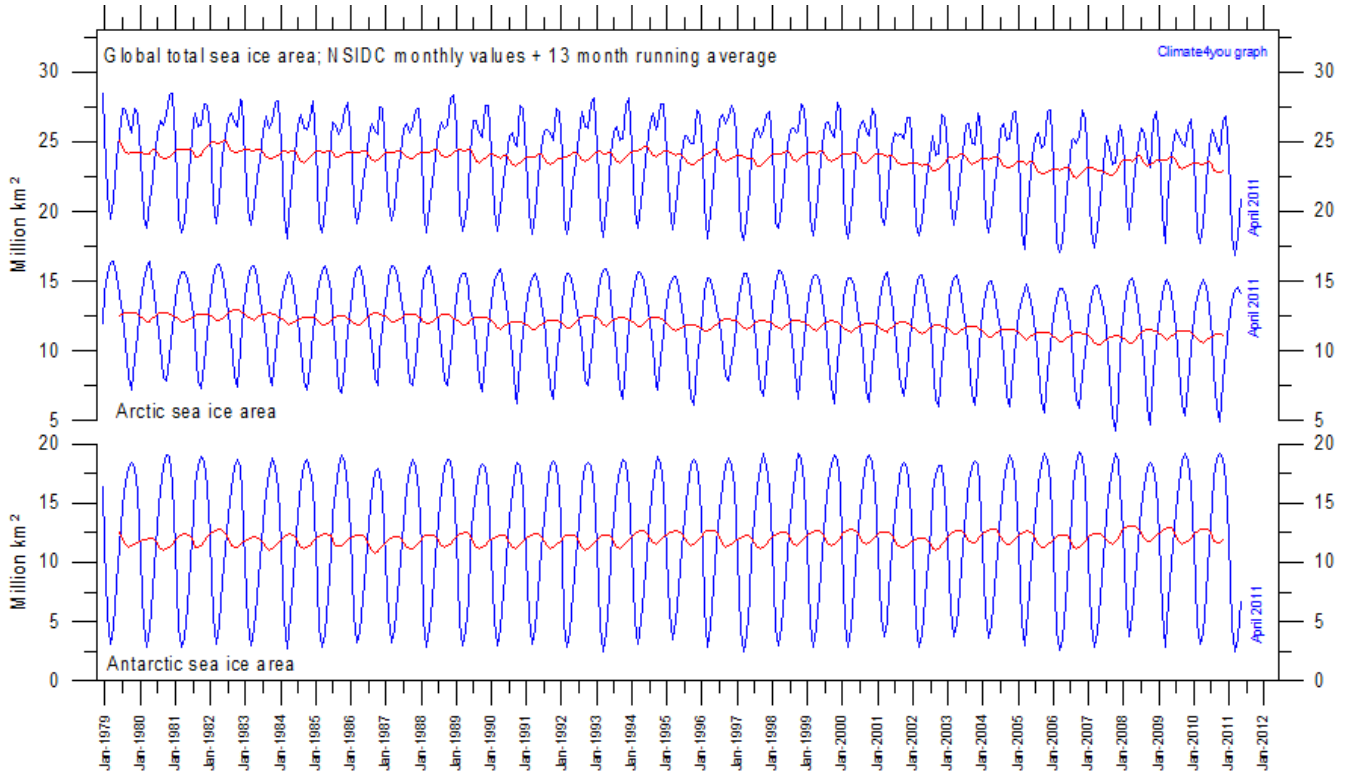
In general, the Arctic temperature record appears to be less variable than the Antarctic record, presumably at least partly due to the higher number of meteorological stations north of 70°N, compared to the number of stations south of 70°S.

As data coverage is sparse in the Polar Regions, the procedure of Gillet et al. 2008 has been followed, giving equal weight to data in each 5°x5° grid cell when calculating means, with no weighting by the areas of the grid cells.

Literature:

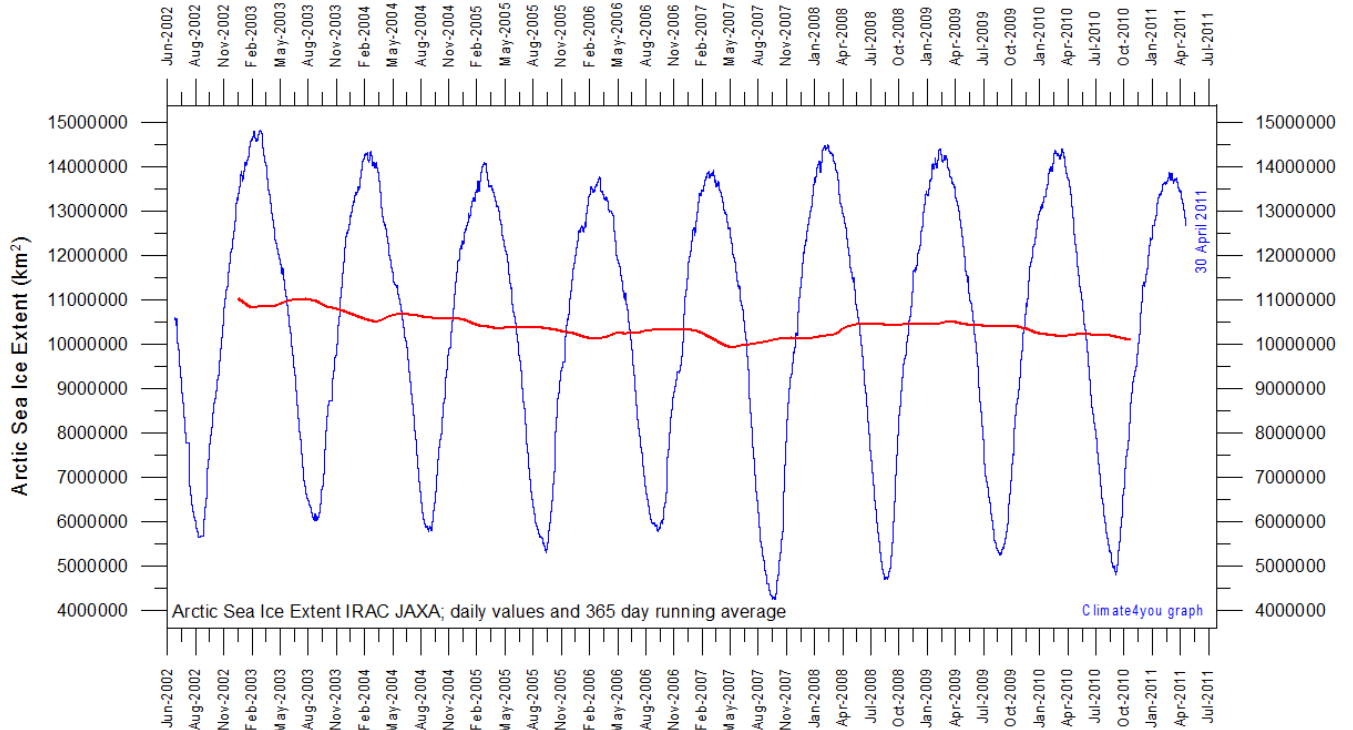
Gillet, N.P., Stone, D.A., Stott, P.A., Nozawa, T., Karpechko, A.Y.U., Hegerl, G.C., Wehner, M.F. and Jones, P.D. 2008. Attribution of polar warming to human influence. *Nature Geoscience* 1, 750-754.

Arctic and Antarctic sea ice, updated to April 2011



16

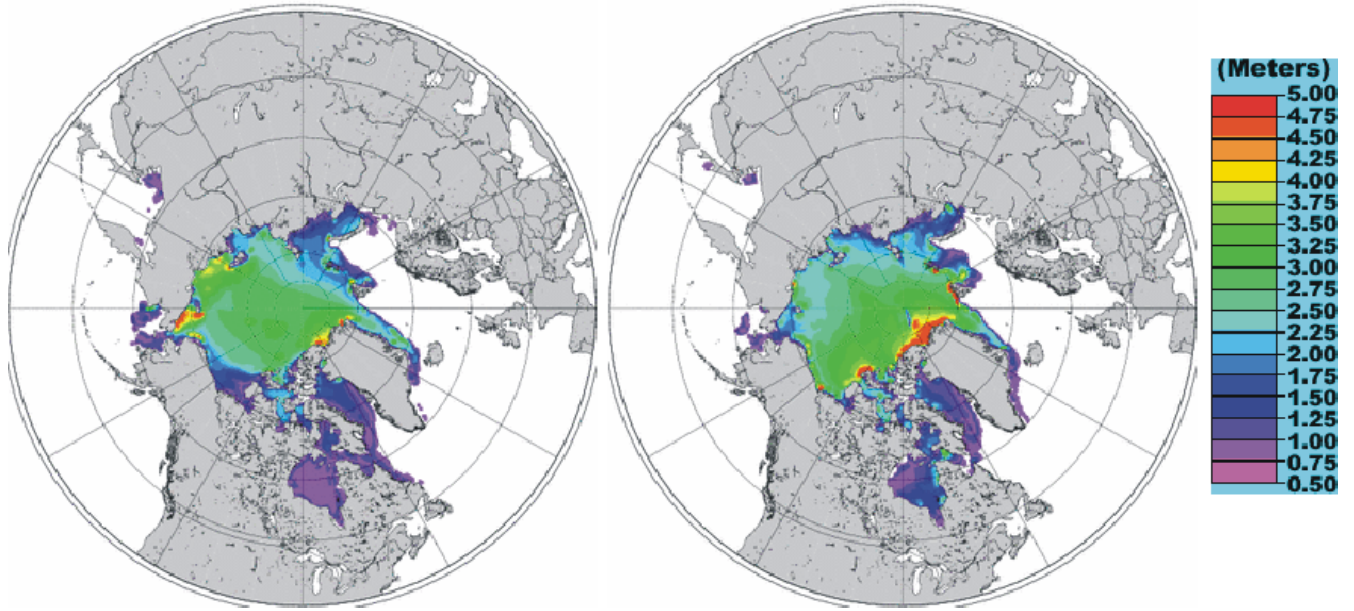
Graphs showing monthly Antarctic, Arctic and global sea ice extent since November 1978, according to the [National Snow and Ice data Center \(NSIDC\)](#).



Graph showing daily Arctic sea ice extent since June 2002, to 30/04 2011, by courtesy of [Japan Aerospace Exploration Agency \(JAXA\)](#).

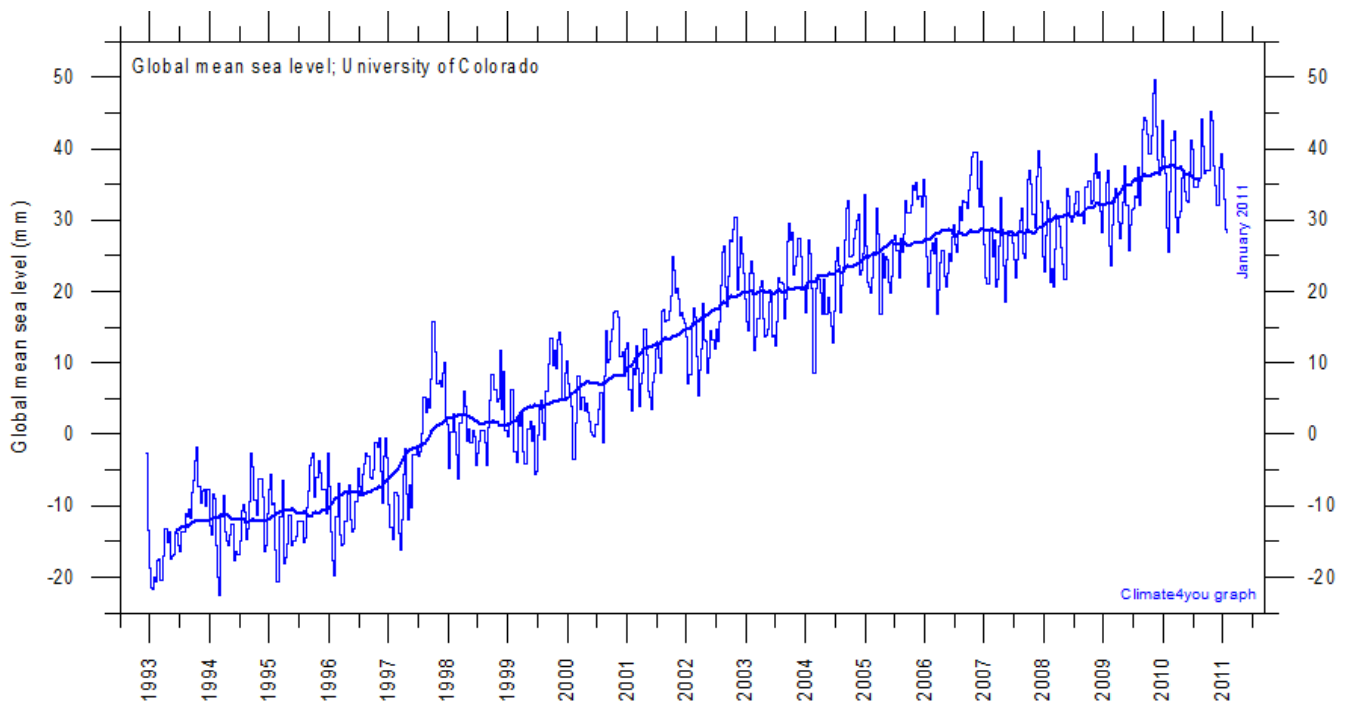
PIPS2.0 24hr forecast from 2010051600_024.dat
valid for 2010051700

PIPS2.0 24hr forecast from 2011051600_024.dat
valid for 2011051700

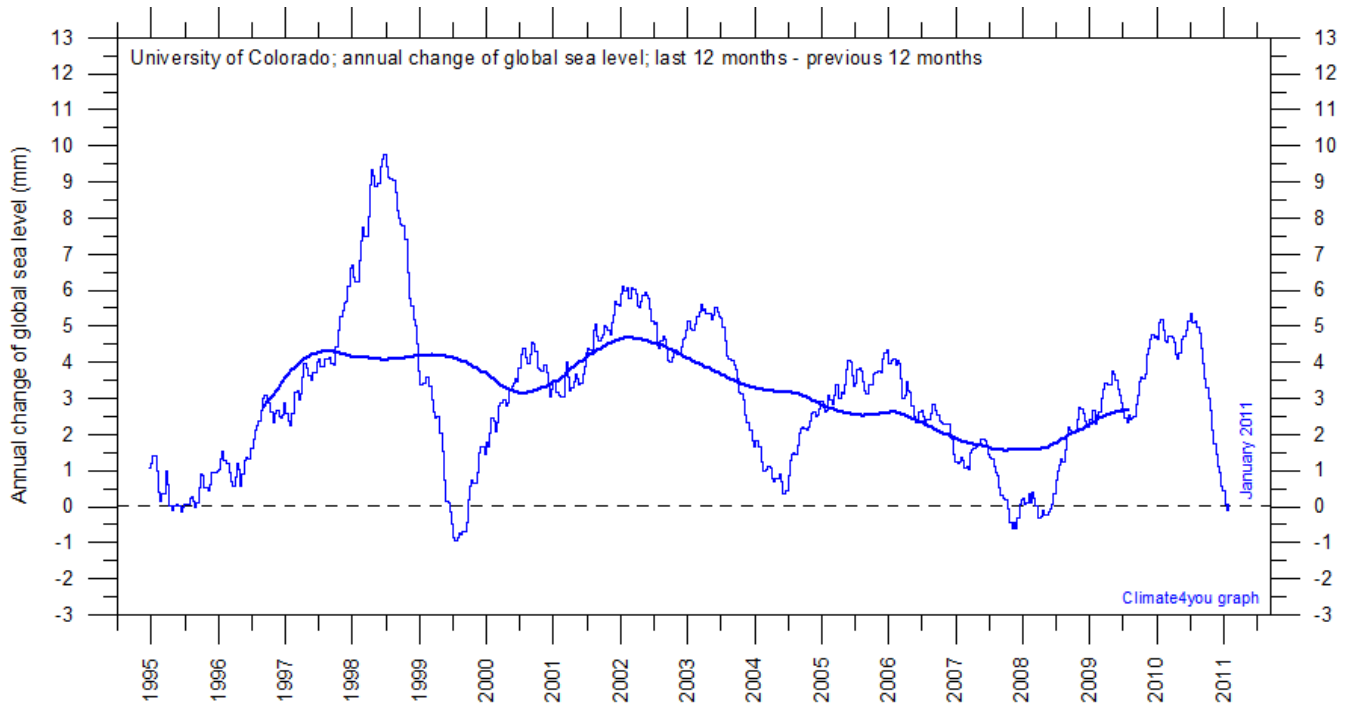


Northern hemisphere sea ice thickness on 17 May 2010 (left) and 2011 (right), according to the Naval Oceanographic Office (NAVO). Thickness values are calculated by the Polar Ice Prediction System (PIPS 2.0), based on the Special Sensor Microwave Image (SSM/I) to initialize the calculation. Thickness scale (m) is shown to the right.

Global sea level, updated to January 2011

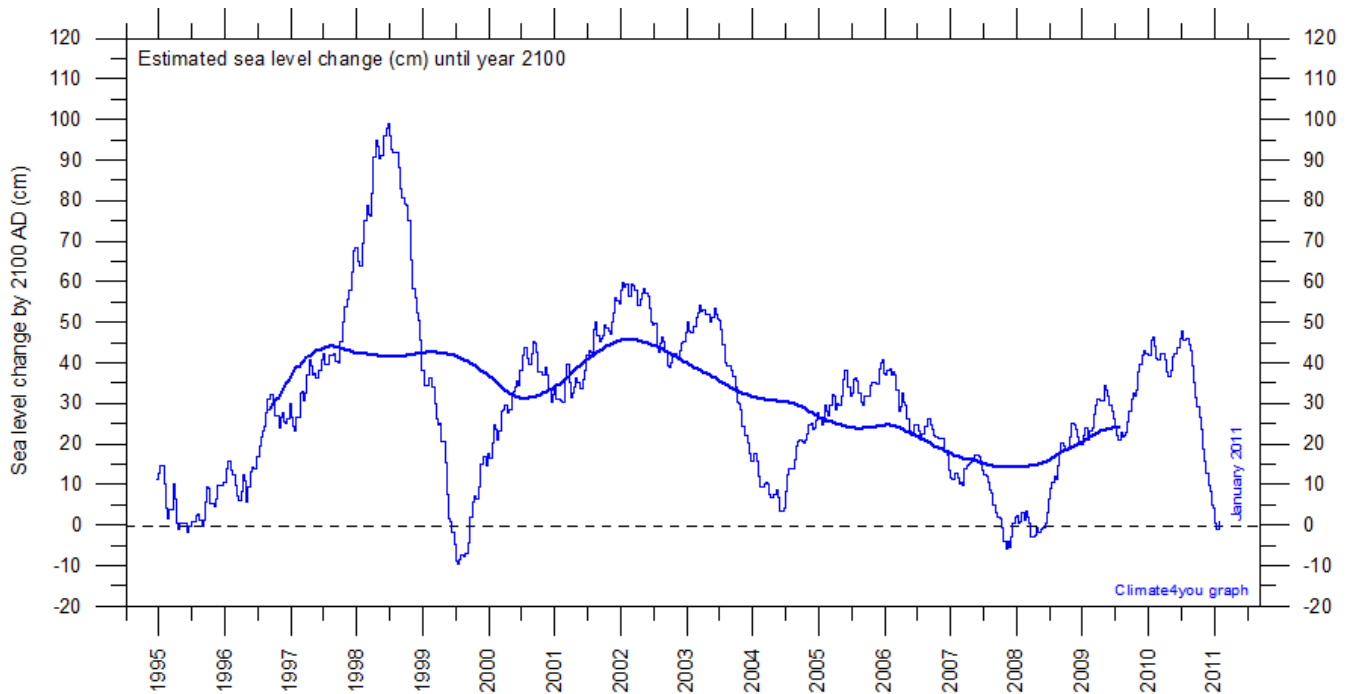


Global monthly sea level since late 1992 according to the Colorado Center for Astrodynamics Research at [University of Colorado at Boulder](#), USA. The thick line is the simple running 37 observation average, nearly corresponding to a running 3 yr average.



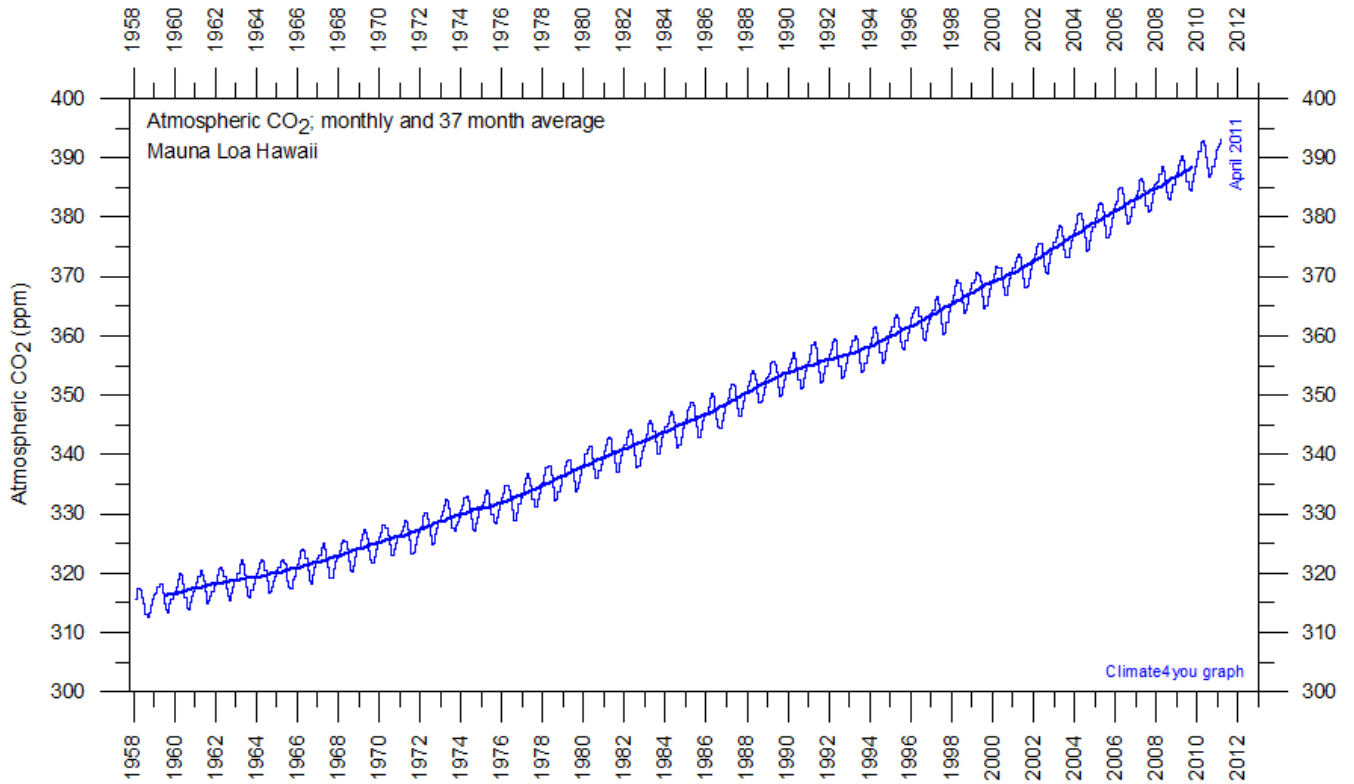
Annual change of global sea level since late 1992 according to the Colorado Center for Astrodynamics Research at [University of Colorado at Boulder](http://www.ccar.colorado.edu), USA. The thick line is the simple running 3 yr average.

18

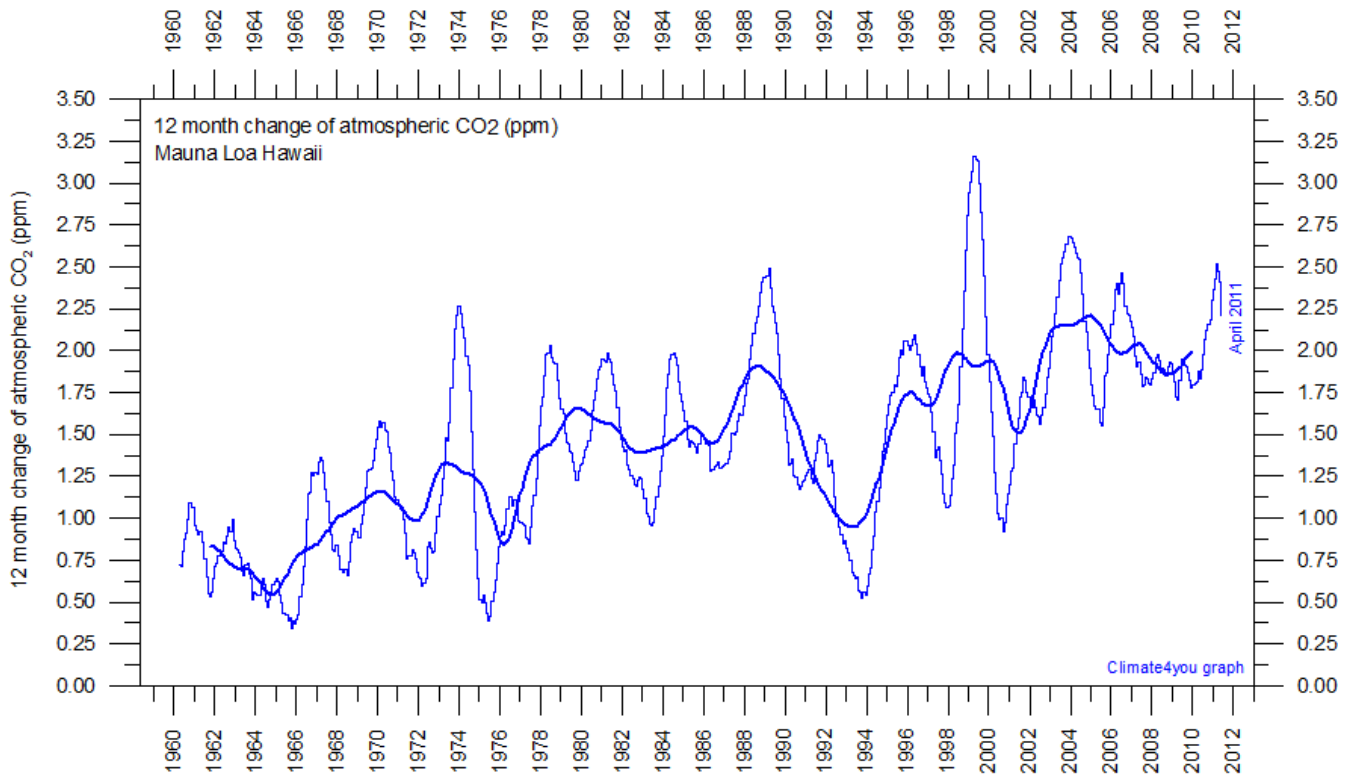


Forecasted change of global sea level until year 2100, based on measurements by the Colorado Center for Astrodynamics Research at [University of Colorado at Boulder](http://www.ccar.colorado.edu), USA. The thick line is the simple running 3 yr average forecast. The present forecast of sea level change until 2100 is 20-25 cm.

Atmospheric CO₂, updated to April 2011

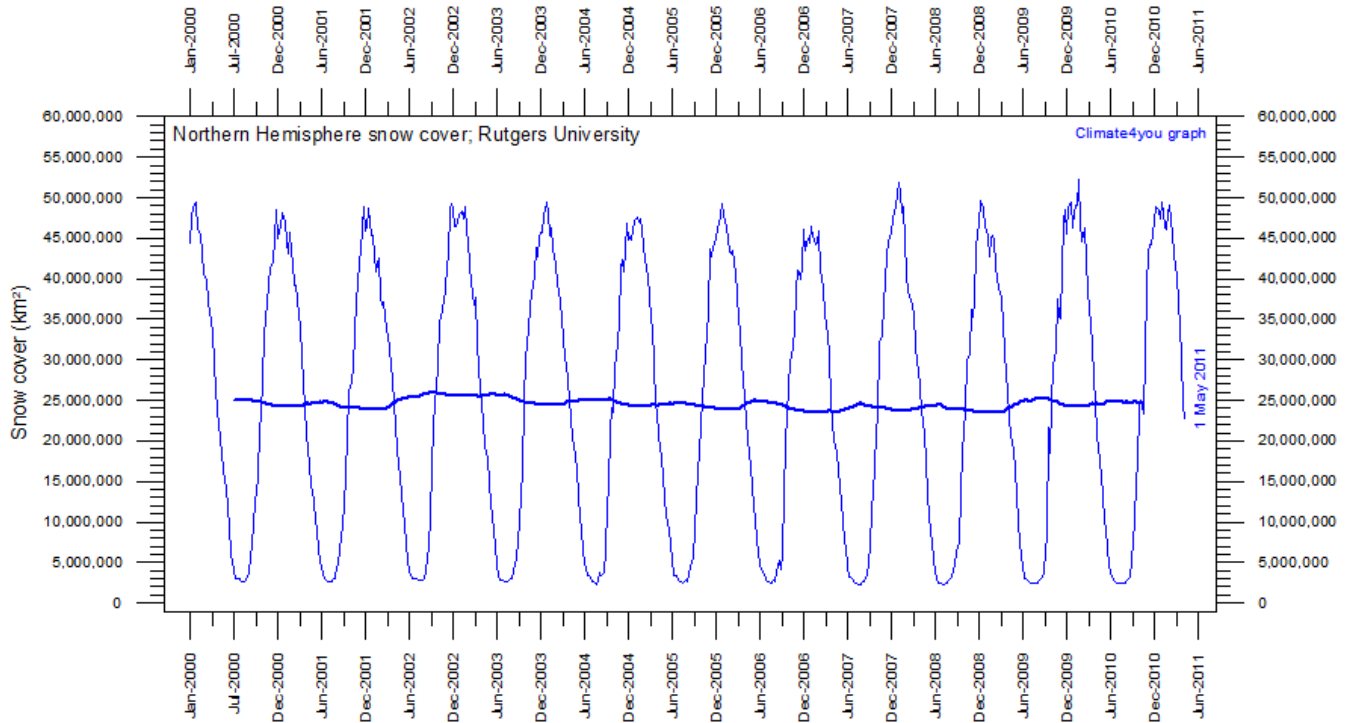


19

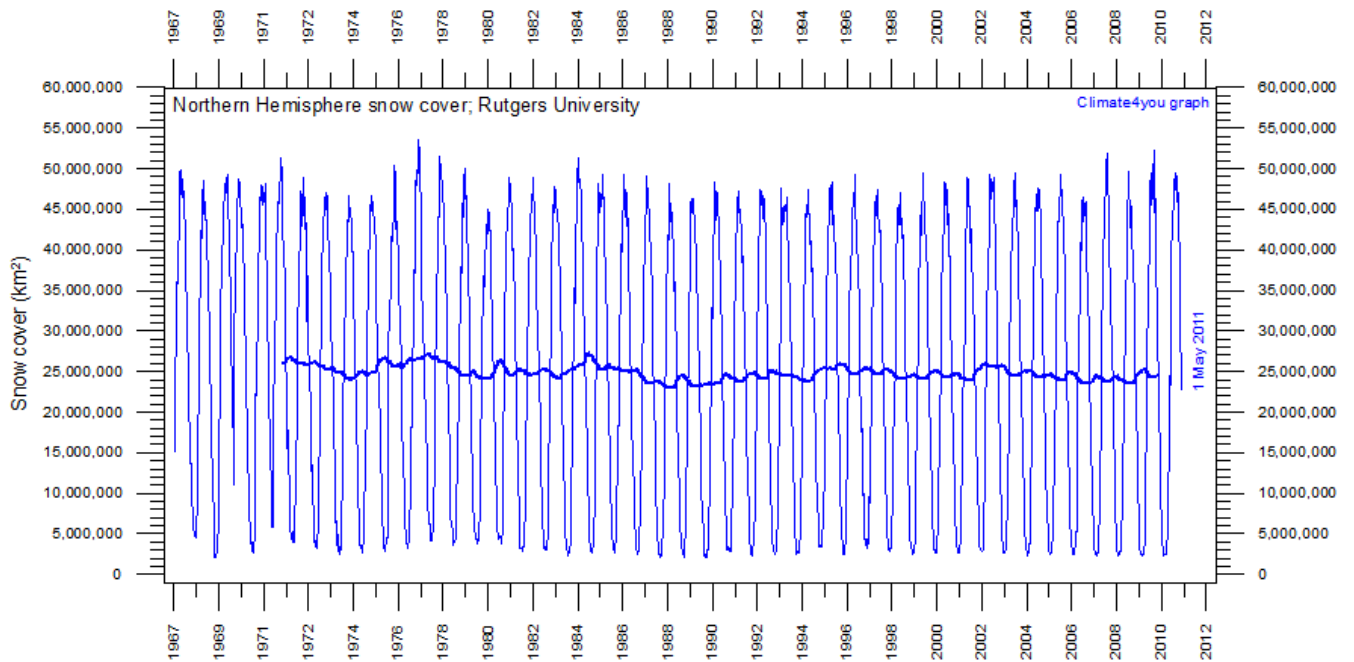


Monthly amount of atmospheric CO₂ (above) and annual growth rate (below; average last 12 months minus average preceding 12 months) of atmospheric CO₂ since 1959, according to data provided by the [Mauna Loa Observatory](#), Hawaii, USA. The thick line is the simple running 37 observation average, nearly corresponding to a running 3 yr average.

Northern Hemisphere weekly snow cover, updated to late April 2011

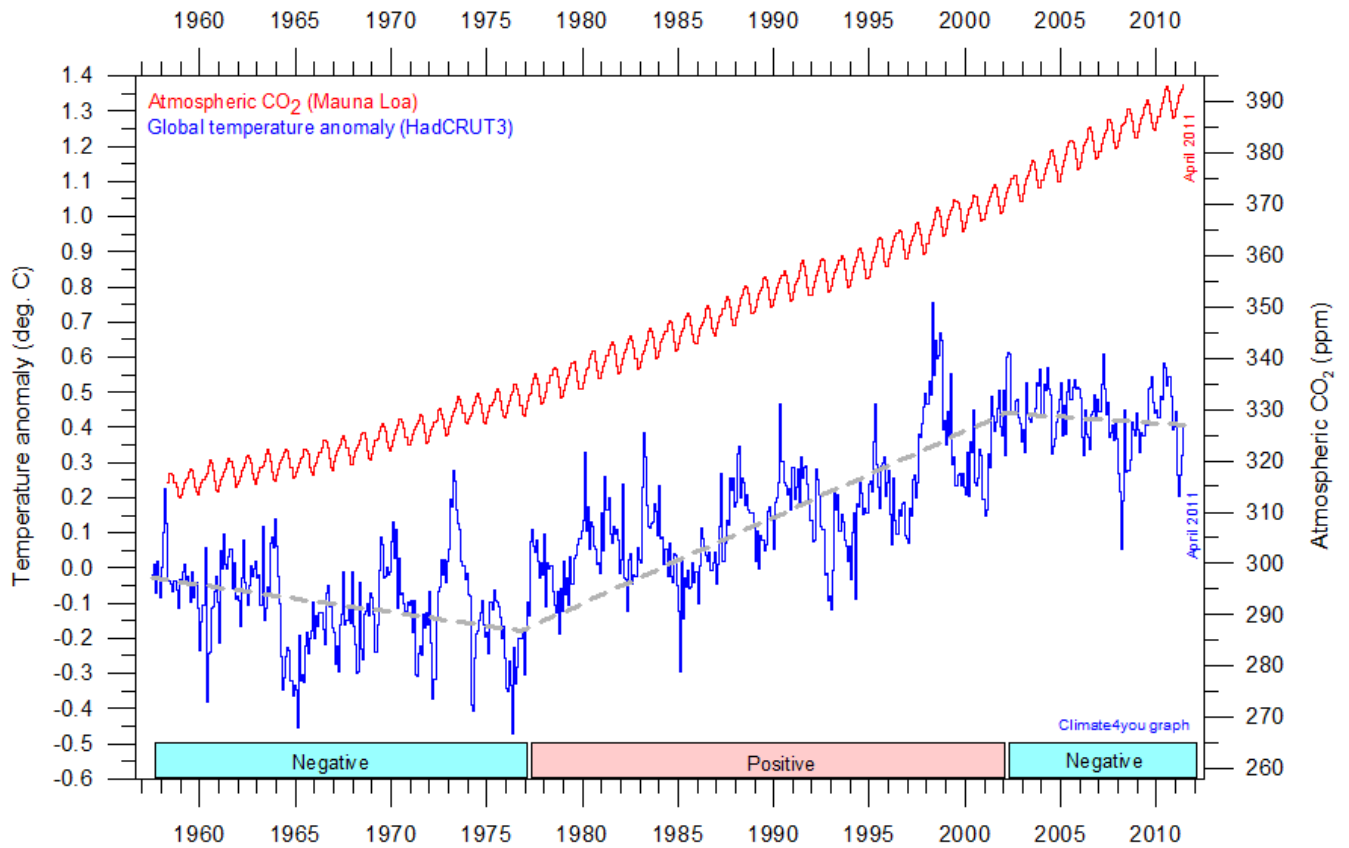


Northern hemisphere weekly snow cover since January 2000 according to Rutgers University Global Snow Laboratory. The thin line is the weekly data, and the thick line is the running 53 week average (approximately 1 year).

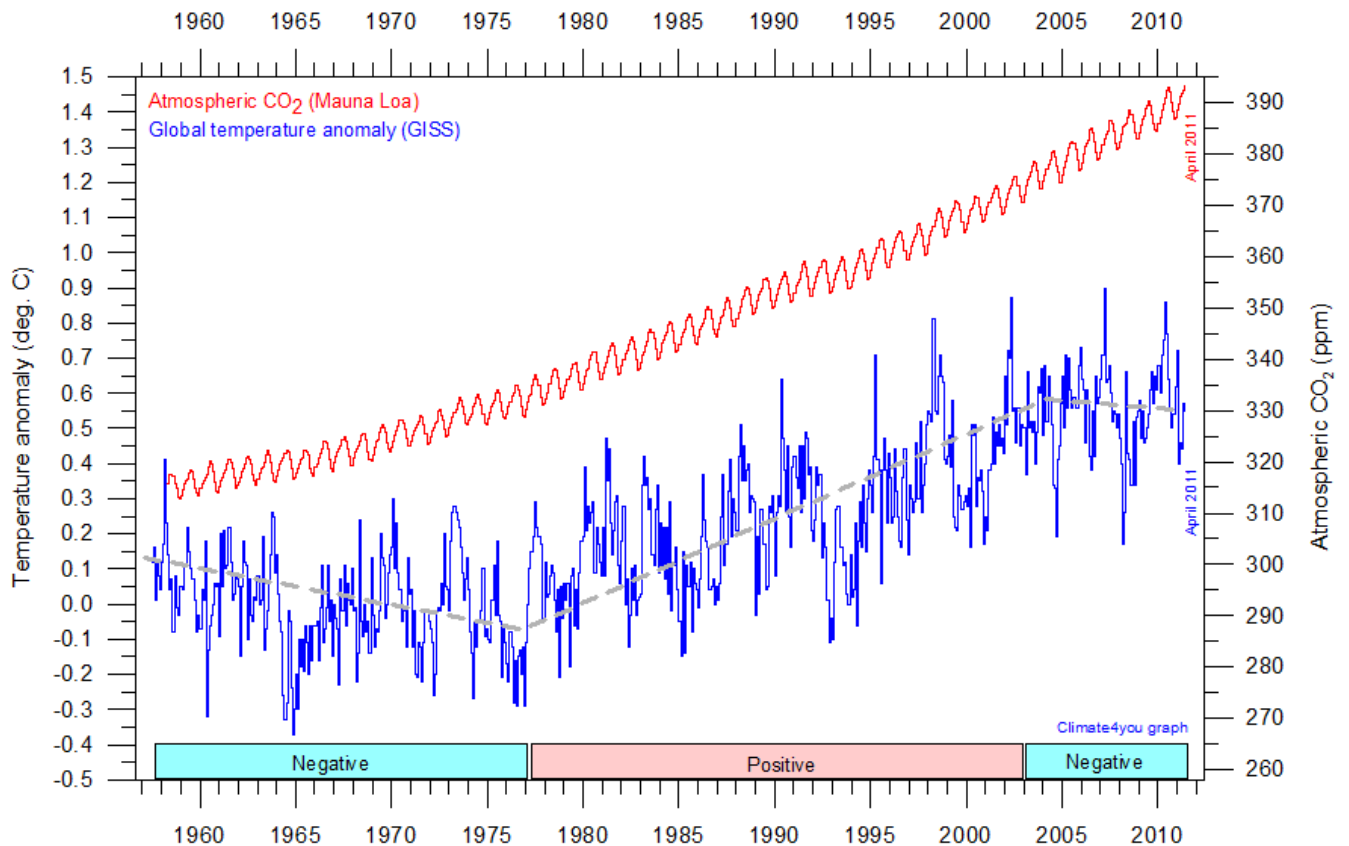


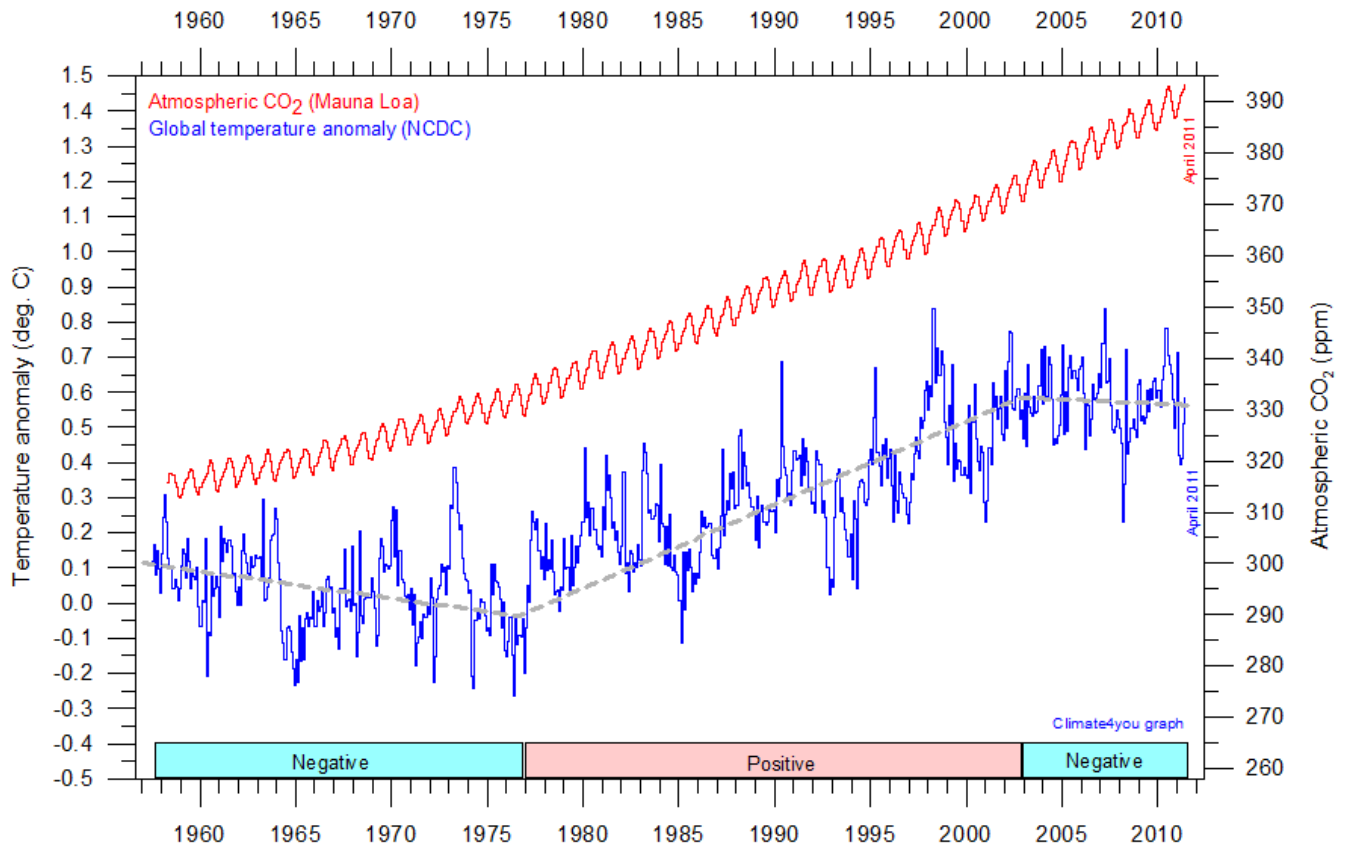
Northern hemisphere weekly snow cover since October 1966 according to Rutgers University Global Snow Laboratory. The thin line is the weekly data, and the thick line is the running 53 week average (approximately 1 year). The running average is not calculated before 1971 because of some data irregularities in this early period.

Global surface air temperature and atmospheric CO₂, updated to April 2011



21





Diagrams showing HadCRUT3, GISS, and NCDC monthly global surface air temperature estimates (blue) and the monthly atmospheric CO₂ content (red) according to the [Mauna Loa Observatory](#), Hawaii. The Mauna Loa data series begins in March 1958, and 1958 has therefore been chosen as starting year for the diagrams. Reconstructions of past atmospheric CO₂ concentrations (before 1958) are not incorporated in this diagram, as such past CO₂ values are derived by other means (ice cores, stomata, or older measurements using different methodology, and therefore are not directly comparable with modern atmospheric measurements). The dotted grey line indicates the approximate linear temperature trend, and the boxes in the lower part of the diagram indicate the relation between atmospheric CO₂ and global surface air temperature, negative or positive.

Most climate models assume the greenhouse gas carbon dioxide CO₂ to influence significantly upon global temperature. Thus, it is relevant to compare the different global temperature records with measurements of atmospheric CO₂, as shown in the diagrams above. Any comparison, however, should not be made on a monthly or annual basis, but for a longer time period, as other effects (oceanographic, clouds, volcanic, etc.) may well override the potential influence of CO₂ on short time scales such as just a few years.

It is of cause equally inappropriate to present new meteorological record values, whether daily, monthly or annual, as support for the hypothesis ascribing high importance of atmospheric CO₂ for global temperatures. Any such short-period meteorological record value may well be the result of other phenomena than atmospheric CO₂.

What exactly defines the critical length of a relevant time period to consider for evaluating the alleged high importance of CO₂ remains elusive, and is still a topic for debate. The critical period length must, however, be inversely proportional to the importance of CO₂ on the global temperature, including feedback effects, such as

assumed by most climate models. So if the effect of CO₂ is strong, the length of the critical period is short, and vice versa.

After about 10 years of global temperature increase following global cooling 1940-1978, IPCC was established in 1988. Presumably, several scientists interested in climate then felt intuitively that their empirical and theoretical understanding of climate dynamics was sufficient to conclude about the high importance of CO₂ for global temperature. However, for obtaining public and political support for the CO₂-hypothesis the 10 year warming period leading up to 1988 in all likelihood was important. Had the global temperature instead been decreasing, public support for the hypothesis would have been difficult to obtain. Adopting this approach as to critical time length, the varying relation (positive or negative) between global temperature and atmospheric CO₂ has been indicated in the lower panels of the three diagrams above.

Climate and history; one example among many

1694: The Culbin Sands disaster in northeast Scotland



Scotland with location of Culbin Sands indicated by red arrow (left). Satellite picture and air photo showing Culbin Sands, today covered by forest (dark green, right). The rivers Nairn and Findhorn are seen to the left and right, respectively. The geometry of the coastal barriers (white due to lack of vegetation) shows the net coastal transport to be from NE towards SW (left). This suggests the river Findhorn to be the main sediment source for the sand now accumulated in the Culbin Sands. The picture covers a distance of 20 km from east to west. North is upward to the right, parallel to the border between the two types of pictures. Picture source: Google Earth.

Little more than 300 years ago there was a very fertile and well-cultivated estate on the southern shore of the Moray Firth in northeastern Scotland. It was known as the barony of Culbin. Amidst the various farms of which the property was composed, stood a well-built mansion in which the owner dwelt; and close by was an extensive

orchard, rich in fruit-bearing trees. The Kinnaird family then in possession was distinguished among the gentry of the neighbourhood, and was connected, by blood or marriage, with some of the leading nobility of Scotland. Surrounded by a flourishing tenants on smaller farms, and rejoicing in a fair estate of many hundred acres, it seemed as if nothing could be more secure than the position which the family of Culbin was privileged to enjoy.

In many respects, this part of Scotland enjoys a mild and pleasant climate, sheltered as it is by mountains both to the west and to the south. The number of warm summer days with sun from a clear sky is relatively high due to this topographic setting, and during winter the nearby North Sea ensures that air temperatures seldom drops more than a few degrees below freezing. The mountains also protect against winter storms with westerly wind direction. The area, however, has one climatic weakness: It has little protection against strong winds from N and NW, wind directions often accompanying travelling weather systems (cyclones) on their backside. In combination with huge amounts of sand eroded from glacial deposits inland and being deposited on the coast west and east of the area by the rivers Nairn and Findhorn, this lack of protection against northwesterly winds was to be the background for the major storm disaster in 1694.



Culbin Sands near Kintessack, looking NW on June 2, 2008. The forest in the background delimits the southernmost part of of the sand dune field which extends 2-3 km inland from the coast. The houses in the middle ground are located on the small remnants of the fertile farming areas which barely escaped destruction during the 1694 storm.

The precise data of the 1694 storm is not known, but presumably it was late October or early November, as reports from the frigate S/S Packan at that time indicate a very severe storm with force 11 suggested. In addition, London reported an unbroken 10-day period of N and NW winds with frequent frost, snow and sleet leading up to the end of October 1694. Stavanger in Norway on 31 October reported snow and hail showers, while Copenhagen in Denmark had frost (Lamb 1991).

By the 1694 storm 16 fertile farms and farmland with a total area of 20-30 km² were overwhelmed by moving sand within the Culbin area. The whole area and the buildings were buried with depths of up to 30 m loose sand. Presumably this was not the first storm with problems derived from moving sand, and there has been discussions on the extent of the sand dunes before the disaster. There apparently was another severe episode of blowing sand in the Culbin area on 21 April 1663, and in the autumn of 1676 a NW storm buried the harvest on the westernmost Culbin farms with up to 50-60 cm of sand (Lamb 1991).

Before the 1694 disaster, Culbin was shown on a 17th century map as being on a peninsula between two bays (Edlin 1976). It was at that time a prosperous area, known as 'the Garden', or alternatively 'the Granary', of the county of Moray.

Reports of the disaster tell that it came during the barley harvest, which in the cool summers of the 1690s was probably late, most likely in late October. In upland parts of Scotland, the largely failed harvests of that decade (including 1694) were generally cut later than late October, but presumably in the fertile lowlands along the south shore of Moray Firth the overall situation was more favourable.



Sand dunes near Wellhill, Culbin Sands, looking upwind (NW) on June 2, 2008. The sand dunes in the area are typically 5-25 m high, and extends 12 km parallel to the coast, and to a maximum distance of 3 km inland. The old fertile farmland and farms are still buried beneath the 28 km² sand cover.

Edlin (1976) and Lamb (1991) cites the following accounts from the event: 'At first only fields were invaded by the sand. A ploughman had to leave his plough, while reapers left their stocks of barley. When the returned, both plough and barley were buried for ever. The drift the advanced upon the village, engulfing cottages and the

laird's mansion. The storm continued through the night, and the next morning some of the cottars had to break through the backs of their houses to get out. On the second day of the storm, the people freed their cattle and fled with their belongings to safer ground. Their flight (downwind, SE) was obstructed by the river Findhorn: since its mouth had been blocked by the drifting sand, its waters rose until it could force a new passage to the sea'. When this eventually happened, the water masses swept away the ancient town and harbour of Findhorn on the east bank of the river, shifting the river's month nearly 2 miles eastward to its present position (Chambers 1861). When the population of Culbin returned after the storm, no traces of their houses were to be seen.

Many stories, the product of naturally curious and superstitious minds, developed in the time following the disaster. How could such a disaster befall the once wealthy lands and families of Culbin ? Women were accused of witchcraft and put to death by the Laird who, in turn, was accused of playing cards on a Sunday with the Devil with his estates at stake.



Proximal (upwind) side of 10-15 m high sand dune in central Culbin Sands, looking E on June 2, 2008. The trees growing on top of the dune provides the scale.

For over a hundred years the Culbin Sands remained a sand desert. The land was sold several times and divided into smaller estates. It was, however, not until 1839 that anything was successfully grown on it. Then, Grant of Kincorth, growing marram grass to stabilise the sand planted the first shelter belt to be successful. In 1842 Grigor of Forres, a tree nurseryman, planted 300 acres on Moy Estate. He introduced the technique of 'thatching' to tree planting in Culbin, which turned out to be the key to the ultimate success of planting trees on sand dunes. Branches and tops of trees cut for thinning were laid on the ground, the tree seedlings being planted through the branches. These dead branches remained, holding the sand, protecting the small trees from wind slowing down the evaporation of moisture from the soil. Between 1922 and 1945 the estates constituting

Culbin were acquired by the forestry Commission who, over a period of 32 years, planted over 9000 acres of trees. They stabilised the mobile sand by first planting marram grass whose plexus of spreading roots bound the sand. This was successful on the less hilly terrain but the thatching system, pioneered by Grigor in 1841, was found to be necessary for holding the larger sand dunes. Most of Culbin sands is now afforested.

During the 2nd World War the extensive tidal flats north of Culbin Sands were considered a possible landing area for airplanes and gliders, should Germany attempt an invasion of the British Isles. To prevent this, a large number of wooden poles were dug into the tidal flats. Many of these poles can still be seen. Later in the war, a large part of Culbin and adjacent coastal areas were commandeered by the British Army for manoeuvres in preparation for the D-Day landings. 'Lost' shells and rockets have been found during planting and in 1986 a wrecked aircraft was discovered, having lain undisturbed for 40 years within the dune field.

1966 the Nature Conservancy Council (forerunner of Scottish Natural Heritage) designated the Culbin area a Site of Special Scientific Interest. It also now forms part of a Ramsar site, a Special Protection Area. This unique region is now frequently visited and studied by geologists, botanists and zoologists and other interested parties from around the world.

Lamb (1991) carried out an analysis of the likely meteorological situation leading to the storm destroying the Culbin area, citing, among others, Willis (1986). It is concluded that the fatal 1694 storm winds indeed were blowing from the NW, exposing pre-existing coastal sand dunes to the full force of the wind. At low tide, also the extensive sandy tidal flats (see satellite picture above) beyond the coast would have been exposed to wind erosion, generating additional amounts of wind-blown sand. Finally, excessive plucking of the marram grass on the coastal dunes may have contributed to exposing their surface for wind erosion. That this may have been a contributing factor is indicated by an Act of the Scottish parliament in 1695 (the year after the disaster) forbidding the pulling of marram grass for thatching. However, Lamb (1991) concludes that the winds associated with the 1694 NW storm must have been exceptionally strong, and presumably lasted for about 30 hours without interruption. Gust wind speeds during the storm are estimated to have reached 50-65 m/s, while the mean wind speed may have been around 25-30 m/s.

Edlin (1976) concluded that the new landscape produced by the 1694 storm, today known as the Culbin Sands, probably represents one of the greatest wind-borne deposits formed anywhere in Britain in recent geological time.

Lamb (1991) further draws attention to the fact that this was the time during the Little Ice Age, where the polar pack ice expanded farthest south into the North Atlantic, surrounding Iceland completely by the end of the year. Although the polar waters had long extended further south than what has been normal during the 20th century, the reported swift advance of the polar ice-pack limit between October and December 1694 must have required continual northerly strong winds over much of the North Atlantic north of Iceland. The Culbin Sands may thus be perceived as the geomorphological result of a climatic situation with the oceanic Polar Front taking a very southerly position, in the vicinity of northern Scotland.

References:

Chambers, N. 1861. *Domestic Annals of Scotland*,. vol. iii., pp. 119-120.

Edlin, H.L. 1976. *The Culbin Sands*. In Environment and Man, vol.4, Reclamation (Edited by J. Leniham and W.W. Fletcher), Glasgow and Edinburgh, pp. 1-13.

Lamb, H.H. 1991. *Historical Storms of the North Sea, British Isles and Northwest Europe*. Cambridge University Press, Cambridge, 204 pp.

Willis, D.P. 1986. *Sand and silence - lost villages of the North (Forvie, Rattray, Culbin and Skara Brae)*. Aberdeen University Centre for Scottish Studies, Aberdeen.

All the above diagrams with supplementary information, including links to data sources and previous issues of this newsletter, are available on www.climate4you.com

Yours sincerely, Ole Humlum (Ole.Humlum@geo.uio.no)

19 May 2011.